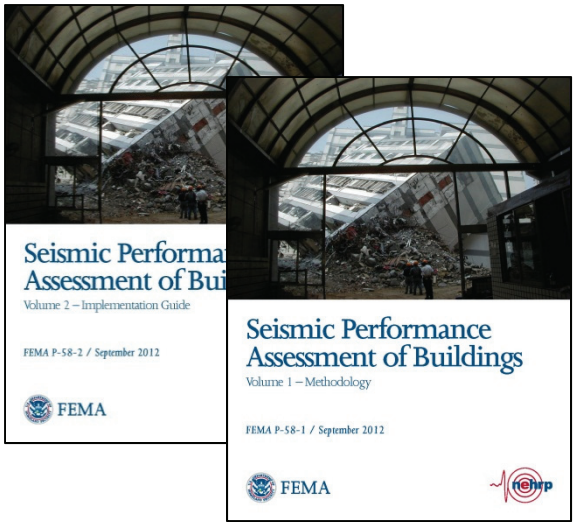

Background Document

FEMA P-58/BD-3.8.8

Damage States and Fragility Curves for Low Aspect Ratio Reinforced Concrete Walls

Prepared by

Kerem Gulec and Andrew Whittaker
University at Buffalo, Buffalo, New York

John Hooper
Magnusson Klemencic Associates, Seattle, Washington

Submitted to

APPLIED TECHNOLOGY COUNCIL
201 Redwood Shores Parkway, Suite 240
Redwood City, California 94065
www.ATCouncil.org

Prepared for

FEDERAL EMERGENCY MANAGEMENT AGENCY
U.S. Department of Homeland Security
500 C Street, SW
Washington, D.C. 20472

October 15, 2009

FEMA

nehrp

Background Documentation

FEMA P-58 Background Documents are a series of reports documenting the technical background and source information for key aspects of the FEMA P-58 methodology and its implementation. These reports were developed over the course of the 10-year ATC-58/ATC-58-1 Projects funded under FEMA Contracts EMW-2001-RP-0056 and HSFEHQ-06-D-1105.

Background Documents were developed by consultants, serving at various levels within the project hierarchy, reporting the results of: (1) decisions on technical development protocols; (2) focused studies on the development of key aspects of the methodology; (3) documentation of recommended procedures; and (4) collection of available data for the development of structural and nonstructural fragilities. They were initially intended to serve as a record of the technical state-of-knowledge at the time they were produced, and as resources for the development of the eventual project reports. As such, they represent a snapshot in time, and may, or may not, match the technical content, recommended procedures, or data incorporated into the final methodology and its implementation.

This Background Document is intended for the purpose of providing supplemental knowledge to users of the FEMA P-58 methodology. Information contained herein has not been independently verified for accuracy as a stand-alone document, and may have been superseded in its final implementation within the methodology. Users of information in this document assume all liability arising from such use.

Notice

Cover illustration – Primary resource documents for the FEMA P-58 *Seismic Performance Assessment of Buildings, Methodology and Implementation* series of products: FEMA P-58-1, *Volume 1 – Methodology*, and FEMA P-58-2, *Volume 2 – Implementation Guide*.

DAMAGE STATES AND FRAGILITY CURVES FOR LOW ASPECT RATIO REINFORCED CONCRETE WALLS

Prepared for the Applied Technology Council
Project ATC-58

Prepared by
Kerem Gulec and Andrew Whittaker, University at Buffalo
John Hooper, Magnusson Klemencic Associates

October 15, 2009

1 Introduction

A general framework for seismic performance assessment and loss computations is provided in the 50% draft of the ATC-58 *Guidelines for Seismic Performance Assessment of Buildings* [ATC (2008)]. A key component of the framework is fragility functions for components and elements of seismic framing systems. Fragility functions relate the probability of exceeding one or more damage thresholds (described using damage states and repair measures) to a demand parameter such as story drift or component plastic deformation. This report summarizes the development of fragility curves for low aspect ratio reinforced concrete walls.

Damage states are characterized typically using descriptors such as concrete crack width, extent of concrete crushing, sliding shear displacement and reinforcement yielding and buckling. However, to compute dollar losses and estimates of building downtime, damage states must be characterized by measures (or scopes) of repair and such descriptions are presented herein. Information is used from experiments on in-plane tests of low aspect ratio (also termed squat, short or low-rise) walls reported in the literature to generate damage data as a function of an efficient demand parameter. Alternate probability distributions are used to present the damage data. Goodness-of-fit tests are performed to evaluate the utility of these distributions. Out-of-plane response of low aspect ratio walls is not considered herein.

2 Summary of Experimental Data

A significant number of low aspect ratio reinforced concrete walls have been tested in the past 60 years. Gulec (2009) assembled a database that includes test results for 434 low aspect ratio reinforced concrete walls. Most of the experimental programs focused on the maximum strength and initial (elastic) stiffness of such walls. The progression of damage with increasing lateral displacement (drift) was of secondary interest. Information that is key to the development of damage states and fragility curves such as maximum crack width, reinforcement yielding and buckling, extent of concrete crushing, and photographs illustrating the condition of specimens at various stages of the experiments were rarely reported. Accordingly, only a fraction of the experimental data reviewed in Gulec (2009) was used to develop fragility functions.

The properties of the test specimens used to develop fragility functions are summarized in Table 1 through Table 6. Specimens are grouped with respect to wall geometry: rectangular, barbell and flanged. In these tables, P is axial force; A is total wall area; f_c' is concrete compressive strength; h_w is wall height; l_w is wall length; t_w is web thickness; b_f and h_f are width and depth of the boundary element, respectively; M/V is moment-to-shear ratio at the base of the wall; ρ_{be} is boundary element reinforcement ratio, ρ_v is vertical web reinforcement ratio, and ρ_h is the horizontal web reinforcement ratio. The column labeled *scale* in Table 2, Table 4 and Table 6 seeks to identify the size of the test specimen with respect to typical building construction by presenting the ratio of web panel thickness to 8 inches. The acronym MoR in these tables denotes Method of Repair, which is defined later in this report.

No	Reference	Wall ID	Loading	P / Af_c' (%)	Number of damage data per MoR			
					1	2	3	4
1	Pilakoutas (1991)	SW4	Cyclic	0.0	1	1	1	1
2		SW5	Cyclic	0.0	1	1	0	1
3		SW6	Cyclic	0.0	1	1	1	1
4		SW7	Cyclic	0.0	1	1	0	1
5		SW8	Cyclic	0.0	1	1	1	1
6		SW9	Cyclic	0.0	1	1	1	1
7	Greifenhagen et al. (2005)	M1	Cyclic	2.2	2	1	1	2
8		M2	Cyclic	2.2	0	1	3	1
9		M3	Cyclic	9.5	2	1	3	1
10		M4	Monotonic	5.0	2	1	3	1
11	Lefas et al. (1990)	SW11	Monotonic	0.0	0	0	0	1
12		SW12	Monotonic	8.7	0	0	0	1
13		SW13	Monotonic	18.1	2	1	1	0
14		SW14	Monotonic	0.0	2	1	1	0
15		SW15	Monotonic	8.8	2	1	1	0
16		SW16	Monotonic	18.0	2	1	1	0
17		SW17	Monotonic	0.0	2	1	1	0
18		SW21	Monotonic	0.0	2	1	1	0
19		SW22	Monotonic	9.1	2	1	1	0
20		SW23	Monotonic	18.2	2	1	1	0
21		SW24	Monotonic	0.0	2	1	1	0
22		SW26	Monotonic	0.0	2	1	1	0
23	Maier and Thürlimann (1985)	S4	Monotonic	6.7	2	1	1	0
24		S9	Cyclic	7.5	2	1	1	0
25	Wiradinata (1985)	Wall-1	Cyclic	0.0	1	3	1	0
26		Wall-2	Cyclic	0.0	1	3	0	1
27	Pilette (1987)	Wall-4	Cyclic	0.0	1	3	2	1
28		Wall-5	Cyclic	0.0	1	3	0	1
29	Mohammadi-Doostdar (1994)	Wall-7	Cyclic	0.0	2	2	0	1
30		Wall-8	Cyclic	0.0	1	2	1	1

Table 1 Summary of rectangular wall data used to create fragility functions

No	Reference	Wall ID	Loading	P / Af_c' (%)	Number of damage data per MoR			
					1	2	3	4
31	Salonikios et al. (1999)	MSW1	Cyclic	0.0	0	0	0	1
32		MSW3	Cyclic	7.0	0	0	0	1
33		MSW6	Cyclic	0.0	0	0	0	1
34		LSW3	Cyclic	7.0	0	0	0	1
35	Synge (1980)	Wall-1	Cyclic	0.0	1	3	2	1
36	Massone (2006)	wp111-9	Cyclic	10.0	1	3	0	1
37		wp111-10	Cyclic	10.0	1	3	0	1
38		wp1105-8	Cyclic	5.0	1	3	0	1
39		wp1105-7	Cyclic	5.0	1	3	0	1
40		wp110-5	Cyclic	0.0	0	3	0	1
41		wp110-6	Monotonic	0.0	0	3	0	1
42	Xie and Xiao (2000)	W-1A	Cyclic	9.4	2	0	1	1
43	Hidalgo et al. (2002)	23	Cyclic	0.0	2	1	0	1
44		27	Cyclic	0.0	3	1	0	1
45	Lopes and Elnashai (1991)	SW11	Cyclic	0.0	2	2	1	1
46		SW12	Cyclic	0.0	1	1	1	1
47		SW13	Cyclic	0.0	3	2	0	1
48		SW14	Cyclic	0.0	1	1	0	2
49		SW15	Cyclic	0.0	1	1	1	2
50		SW16	Cyclic	0.0	0	0	0	1
51		SW17	Monotonic	0.0	0	0	0	1

Table 1 Summary of rectangular wall data used to create fragility functions (cont'd)

No	h_w / l_w	M / Vl_w	h_w (in)	l_w (in)	t_w (in)	Scale	b_f (in)	h_f (in)	ρ_{be} (%)	ρ_v (%)	ρ_h (%)	f_c' (psi)
1	2.00	2.13	47.2	23.6	2.36	0.30	2.4	4.3	6.9	0.50	0.39	5352
2	2.00	2.13	47.2	23.6	2.36	0.30	2.4	2.4	12.7	0.59	0.31	4612
3	2.00	2.13	47.2	23.6	2.36	0.30	2.4	4.3	6.9	0.50	0.31	5599
4	2.00	2.13	47.2	23.6	2.36	0.30	2.4	2.4	12.7	0.59	0.39	4641
5	2.00	2.13	47.2	23.6	2.36	0.30	2.4	4.3	7.1	0.50	0.28	6643
6	2.00	2.13	47.2	23.6	2.36	0.30	2.4	4.3	7.1	0.50	0.56	5642
7	0.61	0.69	24.0	39.4	3.94	0.49	0.0	0.0	0.0	0.34	0.37	7352
8	0.61	0.69	24.0	39.4	3.94	0.49	0.0	0.0	0.0	0.34	0.00	7395
9	0.68	0.77	24.0	35.4	3.15	0.39	0.0	0.0	0.0	0.39	0.26	2915
10	0.68	0.77	24.0	35.4	3.15	0.39	0.0	0.0	0.0	0.39	0.26	3538
11	1.00	1.10	29.5	29.5	2.76	0.34	3.9	5.1	8.5	2.14	1.17	7140
12	1.00	1.10	29.5	29.5	2.76	0.34	3.9	5.5	6.5	2.14	1.17	7332
13	1.00	1.10	29.5	29.5	2.76	0.34	2.8	5.5	3.1	2.14	1.17	5423
14	1.00	1.10	29.5	29.5	2.76	0.34	2.8	5.5	3.1	2.14	1.17	5642
15	1.00	1.10	29.5	29.5	2.76	0.34	2.8	5.5	3.1	2.14	1.17	5819
16	1.00	1.10	29.5	29.5	2.76	0.34	2.8	5.5	3.1	2.14	1.17	7052
17	1.00	1.10	29.5	29.5	2.76	0.34	2.8	5.5	3.1	2.14	0.37	6553
18	2.00	2.12	51.2	25.6	2.56	0.32	2.8	5.5	3.1	2.09	0.87	5745
19	2.00	2.12	51.2	25.6	2.56	0.32	2.8	5.5	3.1	2.09	0.87	6891
20	2.00	2.12	51.2	25.6	2.56	0.32	2.6	5.5	3.3	2.09	0.87	6480
21	2.00	2.12	51.2	25.6	2.56	0.32	2.6	5.5	3.3	2.09	0.87	6553
22	2.00	2.12	51.2	25.6	2.56	0.32	2.6	5.5	3.3	2.09	0.40	3881
23	1.02	1.12	47.2	46.5	3.94	0.49	2.6	5.5	3.3	1.02	1.01	4772
24	1.02	1.12	47.2	46.5	3.94	0.49	2.6	5.5	3.3	1.02	0.00	4235
25	0.50	0.58	39.4	78.7	3.94	0.49	0.0	0.0	0.0	0.59	0.26	3626
26	0.25	0.33	19.7	78.7	3.94	0.49	0.0	0.0	0.0	0.59	0.26	3191
27	0.50	0.58	39.4	78.7	3.94	0.49	3.9	12.6	1.3	0.59	0.80	4786
28	0.50	0.58	39.4	78.7	3.94	0.49	3.9	12.6	1.3	1.07	1.20	3916
29	0.75	0.82	59.1	78.7	3.94	0.49	3.9	12.6	1.3	0.59	0.80	6527
30	1.00	1.09	59.1	59.1	3.94	0.49	3.9	9.8	1.6	0.51	0.80	6527

Table 2 Geometric and material properties of the rectangular wall data

No	h_w / l_w	M / Vl_w	h_w (in)	l_w (in)	t_w (in)	Scale	b_f (in)	h_f (in)	ρ_{be} (%)	ρ_v (%)	ρ_h (%)	f'_c (psi)
31	1.50	1.60	70.9	47.2	3.94	0.49	3.9	9.4	1.7	0.57	0.57	3785
32	1.50	1.60	70.9	47.2	3.94	0.49	3.9	9.4	1.3	0.28	0.28	3495
33	1.50	1.60	70.9	47.2	3.94	0.49	3.9	9.4	1.7	0.57	0.57	3988
34	1.00	1.10	47.2	47.2	3.94	0.49	3.9	9.4	1.3	0.57	0.57	3219
35	0.50	0.57	59.1	118.1	3.94	0.49	3.9	9.4	1.9	0.81	1.61	3945
36	0.89	0.44	48.0	54.0	6.00	0.75	6.0	7.5	0.9	0.25	0.27	4100
37	0.89	0.44	48.0	54.0	6.00	0.75	6.0	7.5	0.9	0.25	0.27	4550
38	0.89	0.44	48.0	54.0	6.00	0.75	6.0	7.5	0.9	0.25	0.27	4630
39	0.89	0.44	48.0	54.0	6.00	0.75	6.0	7.5	0.9	0.25	0.27	4640
40	0.89	0.44	48.0	54.0	6.00	0.75	6.0	7.5	0.9	0.25	0.27	4340
41	0.89	0.44	48.0	54.0	6.00	0.75	6.0	7.5	0.9	0.25	0.27	4500
42	0.50	0.59	48.0	96.0	6.00	0.75	0.0	0.0	0.0	0.37	0.31	4250
43	1.38	0.69	70.9	51.2	3.94	0.49	1.8	3.1	5.9	0.00	0.25	3655
44	1.00	0.50	55.1	55.1	3.94	0.49	1.8	3.1	5.9	0.00	0.25	3597
45	1.90	1.10	33.7	17.7	1.77	0.22	1.8	3.1	5.9	0.39	0.92	6230
46	1.90	1.10	33.7	17.7	1.77	0.22	1.8	3.1	5.9	0.39	0.92	6421
47	1.90	1.10	33.7	17.7	1.77	0.22	1.8	3.1	5.9	0.39	0.92	7537
48	1.90	1.10	33.7	17.7	1.77	0.22	1.8	3.1	5.9	0.39	0.92	6289
49	1.90	1.10	33.7	17.7	1.77	0.22	1.8	3.1	5.9	0.39	0.51	6436
50	1.90	1.10	33.7	17.7	1.77	0.22	3.9	9.4	1.7	0.00	0.62	5995
51	1.90	1.10	33.7	17.7	1.77	0.22	3.9	9.4	1.3	0.00	0.80	6083
Min	0.25	0.33	19.7	17.7	1.77	0.22	0.0	0.0	0.0	0.00	0.00	2915
Max	2.00	2.13	70.9	118.1	6.00	0.75	6.0	14.2	12.7	2.14	1.61	7537
Mean	1.27	1.15	43.3	41.7	3.41	0.43	2.9	5.6	3.3	0.83	0.61	5249

Table 2 Geometric and material properties of the rectangular wall data (cont'd)

No	Reference	Wall ID	Loading	P / Af_c' (%)	Number of damage data per MoR			
					1	2	3	4
1	AIJ (1985b)	CW-0.6-1.2-20	Cyclic	5.8	1	1	0	1
2		CW-0.6-0.6-20	Cyclic	6.6	1	1	0	1
3		CW-0.6-0.8-20	Cyclic	4.9	1	1	0	1
4		CW-0.6-1.6-20	Cyclic	5.8	1	0	0	1
5		CW-0.6-2.0-20	Cyclic	5.7	1	0	0	1
6		CW-0.6-1.2-40	Cyclic	12.3	1	0	0	1
7		CW-0.4-1.2-20	Cyclic	5.9	1	0	0	1
8		CW-0.8-1.2-20	Cyclic	5.9	1	0	0	1
9	AIJ (1986c)	CW-0.6-0.6-20a	Cyclic	6.7	2	2	1	1
10		CW-0.6-0.8-20a	Cyclic	6.6	2	3	1	1
11		CW-0.6-1.2-0	Cyclic	0.0	2	3	1	1
12	AIJ (1985a)	CW-0.6-0-20	Cyclic	5.6	2	1	1	1
13		CW-0.6-0.3-20	Cyclic	5.6	2	3	1	1
14		CW-0.6-2.4-20	Cyclic	5.8	2	2	1	1
15		CW-0.6-2.8-20	Cyclic	6.2	2	1	1	1
16		CW-0.6-0-0	Cyclic	0.0	2	1	1	1
17		CW-0.6-0-40	Cyclic	12.4	2	1	1	1
18		CW-0.6-0.6-0	Cyclic	0.0	2	3	1	1
19		CW-0.6-0.6-40	Cyclic	11.5	2	3	1	1
20		CW-0.4-0.6-20	Cyclic	5.8	2	3	1	1
21		CW-0.8-0.6-20	Cyclic	5.8	2	3	1	1
22		CW-0.4-2.0-20	Cyclic	5.8	2	1	1	1
23		CW-0.8-2.0-20	Cyclic	5.7	2	3	1	1
24	AIJ (1986a)	CW-0.6-2-0	Cyclic	0.0	1	0	0	1
25		CW-0.6-2-40	Cyclic	11.6	1	0	0	1
26		CW-0.6-2-20B	Cyclic	5.5	1	0	0	1
27		CW-0.6-0.6-20L	Cyclic	7.8	1	0	0	1
28		CW-0.6-1.2-20L	Cyclic	7.6	1	0	0	1
29		CW-0.6-2-20L	Cyclic	7.8	1	0	0	1
30	AIJ (1986b)	No1	Cyclic	7.2	0	0	0	1
31		No2	Cyclic	5.1	0	0	0	1
32		No3	Cyclic	3.4	0	0	0	1

Table 3 Summary of barbell wall data used to create fragility functions

No	h_w / l_w	M / Vl_w	h_w (in)	l_w (in)	t_w (in)	Scale	b_f (in)	h_f (in)	ρ_{be} (%)	ρ_v (%)	ρ_h (%)	f'_c (psi)
1	0.46	0.52	41.3	90.6	3.15	0.39	11.8	11.8	1.0	1.20	1.20	4935
2	0.46	0.52	41.3	90.6	3.15	0.39	11.8	11.8	1.0	0.60	0.60	4281
3	0.46	0.52	41.3	90.6	3.15	0.39	11.8	11.8	1.0	0.80	0.80	5760
4	0.46	0.52	41.3	90.6	3.15	0.39	11.8	11.8	1.4	1.60	1.60	4878
5	0.46	0.52	41.3	90.6	3.15	0.39	11.8	11.8	1.8	2.00	2.00	5021
6	0.46	0.52	41.3	90.6	3.15	0.39	11.8	11.8	1.0	1.20	1.20	4608
7	0.28	0.35	25.6	90.6	3.15	0.39	11.8	11.8	1.0	1.20	1.20	4793
8	0.63	0.70	57.1	90.6	3.15	0.39	11.8	11.8	1.0	1.20	1.20	4850
9	0.46	0.52	41.3	90.6	3.15	0.39	11.8	11.8	1.0	0.60	0.60	4224
10	0.46	0.52	41.3	90.6	3.15	0.39	11.8	11.8	1.0	0.80	0.80	4295
11	0.46	0.52	41.3	90.6	3.15	0.39	11.8	11.8	1.0	1.20	1.20	4167
12	0.46	0.52	41.3	90.6	3.15	0.39	11.8	11.8	1.0	0.00	0.00	5106
13	0.46	0.52	41.3	90.6	3.15	0.39	11.8	11.8	1.0	0.30	0.30	5106
14	0.46	0.52	41.3	90.6	3.15	0.39	11.8	11.8	1.8	2.40	2.40	4878
15	0.46	0.52	41.3	90.6	3.15	0.39	11.8	11.8	1.8	2.80	2.80	4594
16	0.46	0.52	41.3	90.6	3.15	0.39	11.8	11.8	1.0	0.00	0.00	4594
17	0.46	0.52	41.3	90.6	3.15	0.39	11.8	11.8	1.0	0.00	0.00	4594
18	0.46	0.52	41.3	90.6	3.15	0.39	11.8	11.8	1.0	0.60	0.60	5106
19	0.46	0.52	41.3	90.6	3.15	0.39	11.8	11.8	1.0	0.60	0.60	4935
20	0.28	0.35	25.6	90.6	3.15	0.39	11.8	11.8	1.0	0.60	0.60	4878
21	0.63	0.70	57.1	90.6	3.15	0.39	11.8	11.8	1.0	0.60	0.60	4864
22	0.28	0.35	25.6	90.6	3.15	0.39	11.8	11.8	1.8	2.00	2.00	4935
23	0.63	0.70	57.1	90.6	3.15	0.39	11.8	11.8	1.8	2.00	2.00	4978
24	0.46	0.52	41.3	90.6	3.15	0.39	11.8	11.8	1.8	2.00	2.00	4893
25	0.46	0.52	41.3	90.6	3.15	0.39	11.8	11.8	1.8	2.00	2.00	4921
26	0.46	0.52	41.3	90.6	3.15	0.39	11.8	11.8	1.0	2.00	2.00	5149
27	0.46	0.52	41.3	90.6	3.15	0.39	11.8	11.8	1.0	0.60	0.60	3655
28	0.46	0.52	41.3	90.6	3.15	0.39	11.8	11.8	1.0	1.20	1.20	3755
29	0.46	0.52	41.3	90.6	3.15	0.39	11.8	11.8	1.8	2.00	2.00	3655
30	0.48	0.55	41.3	85.8	3.15	0.39	7.1	7.1	2.9	1.20	1.20	3940
31	0.48	0.55	41.3	85.8	3.15	0.39	7.1	7.1	2.9	1.20	1.20	5561
32	0.48	0.55	41.3	85.8	3.15	0.39	7.1	7.1	2.9	1.20	1.20	8463
Min	0.28	0.35	25.6	85.8	3.15	0.39	7.1	7.1	1.0	0.00	0.00	3655
Max	0.63	0.70	57.1	90.6	3.15	0.39	11.8	11.8	2.9	2.80	2.80	8463
Mean	0.46	0.52	41.3	90.1	3.15	0.39	11.4	11.4	1.4	1.18	1.18	4824

Table 4 Geometric and material properties of the barbell wall data

No	Reference	Wall ID	Loading	P / Af_c' (%)	Number of damage data per MoR			
					1	2	3	4
1	Barda (1972)	B1-1	Monotonic	0.0	4	2	1	0
2		B2-1	Monotonic	0.0	4	2	1	1
3		B3-2	Cyclic	0.0	4	1	1	1
4		B4-3	Cyclic	0.0	4	2	1	1
5		B5-4	Cyclic	0.0	2	2	1	0
6		B6-4	Cyclic	0.0	4	3	1	1
7		B7-5	Cyclic	0.0	3	3	1	1
8		B8-5	Cyclic	0.0	3	3	1	1
9	Maier and Thürlimann (1985)	S1	Monotonic	6.6	1	3	1	1
10		S2	Monotonic	24.2	2	1	1	1
11		S3	Monotonic	6.5	1	3	0	1
12		S5	Cyclic	6.3	1	4	1	1
13		S6	Monotonic	6.6	1	4	1	1
14		S7	Cyclic	27.3	2	1	0	1
15	Synge (1980)	Wall-3	Cyclic	0.0	1	2	2	1
16	Kitada et al. (1997)	U-1	ES	3.9	0	0	0	1
17	Palermo and Vecchio (2002)	DP1	Cyclic	5.4	3	3	1	1
18		DP2	Cyclic	0.0	3	2	1	1
19	Saito et al. (1989)	W12-1	Cyclic	5.6	1	1	0	1
20	Sato et al. (1989)	24M 8-30	Cyclic	5.3	0	1	1	0
21		24M 8-40	Cyclic	5.6	0	1	1	0
22		24M 8-50	Cyclic	5.7	0	1	1	0
23		36M 8-30	Cyclic	5.1	2	2	1	1
24		36M 8-40	Cyclic	5.2	0	1	1	0
25		36M 8-50	Cyclic	5.3	2	2	1	1
26		48M 8-30	Cyclic	7.3	0	1	1	0
27		48M 8-40	Cyclic	7.3	0	1	1	0
28		48M 8-50	Cyclic	7.1	0	1	1	0

Table 5 Summary of flanged wall data used to create fragility functions

No	h_w / l_w	M / Vl_w	h_w (in)	l_w (in)	t_w (in)	Scale	b_f (in)	h_f (in)	ρ_{be} (%)	ρ_v (%)	ρ_h (%)	f'_c (psi)
1	0.46	0.50	34.5	75.0	4.00	0.50	24.0	4.0	1.8	0.50	0.48	4200
2	0.46	0.50	34.5	75.0	4.00	0.50	24.0	4.0	6.4	0.50	0.48	2370
3	0.46	0.50	34.5	75.0	4.00	0.50	24.0	4.0	4.1	0.50	0.48	3920
4	0.46	0.50	34.5	75.0	4.00	0.50	24.0	4.0	4.1	0.50	0.00	2760
5	0.46	0.50	34.5	75.0	4.00	0.50	24.0	4.0	4.1	0.00	0.48	4190
6	0.46	0.50	34.5	75.0	4.00	0.50	24.0	4.0	4.1	0.26	0.48	3080
7	0.21	0.25	15.8	75.0	4.00	0.50	24.0	4.0	4.1	0.50	0.49	3730
8	0.96	1.00	72.0	75.0	4.00	0.50	24.0	4.0	4.1	0.50	0.50	3400
9	1.02	1.12	47.2	46.5	3.94	0.49	15.7	3.9	1.1	1.13	1.01	5352
10	1.02	1.12	47.2	46.5	3.94	0.49	15.7	3.9	1.1	1.13	1.01	5568
11	1.02	1.12	47.2	46.5	3.94	0.49	15.7	3.9	2.5	2.54	1.01	5323
12	1.02	1.12	47.2	46.5	3.94	0.49	15.7	3.9	1.1	1.13	1.01	5410
13	1.02	1.12	47.2	46.5	3.94	0.49	15.7	3.9	1.1	1.13	0.57	5163
14	1.02	1.12	47.2	46.5	3.94	0.49	15.7	3.9	1.1	1.13	1.01	4946
15	0.50	0.57	59.1	118.1	3.94	0.49	19.7	3.9	1.8	0.37	1.61	3771
16	0.65	0.77	79.5	122.0	2.95	0.37	117.3	3.9	0.5	1.20	1.20	4153
17	0.66	0.76	79.5	121.1	2.95	0.37	119.9	3.7	0.4	0.82	0.76	3147
18	0.65	0.76	79.5	121.5	2.95	0.37	119.9	3.9	0.4	0.82	0.76	2727
19	0.35	0.47	29.5	83.5	4.72	0.59	19.7	4.7	4.8	1.32	1.32	5106
20	0.65	0.74	55.1	84.6	5.91	0.74	39.4	5.9	0.8	0.80	0.80	5512
21	0.65	0.74	55.1	84.6	5.91	0.74	39.4	5.9	0.6	0.60	0.60	5192
22	0.65	0.74	55.1	84.6	5.91	0.74	39.4	5.9	0.5	0.48	0.48	5076
23	0.65	0.74	55.1	84.6	5.91	0.74	39.4	5.9	1.2	1.16	1.16	5700
24	0.65	0.74	55.1	84.6	5.91	0.74	39.4	5.9	0.9	0.90	0.90	5628
25	0.65	0.74	55.1	84.6	5.91	0.74	39.4	5.9	0.7	0.72	0.72	5439
26	0.65	0.74	55.1	84.6	5.91	0.74	39.4	5.9	1.6	1.60	1.60	3974
27	0.65	0.74	55.1	84.6	5.91	0.74	39.4	5.9	1.2	1.16	1.16	3989
28	0.65	0.74	55.1	84.6	5.91	0.74	39.4	5.9	1.0	0.96	0.96	4061
Min	0.21	0.25	15.8	46.5	2.95	0.37	15.7	3.7	0.4	0.00	0.00	2370
Max	1.02	1.12	79.5	122.0	5.91	0.74	119.9	5.9	6.4	2.54	1.61	5700
Mean	0.67	0.75	50.1	78.8	4.51	0.56	37.0	4.6	2.0	0.87	0.82	4389

Table 6 Geometric and material properties of the flanged wall data

The following were common to all specimens listed in Table 1 through Table 6: a) no openings (solid walls); b) symmetric rebar layout; c) no diagonal rebar or additional wall-to-foundation rebar to control sliding shear; d) aspect ratios (h_w / l_w) of less than or equal to 2.0; and e) cantilever test fixture where lateral load is applied to a beam constructed at the top of the wall and the load is transferred to a foundation element anchored to a laboratory floor.

Experimental data from 111 squat walls that met the above criteria provided the damage data presented below. Twenty-eight walls had flanges, 32 walls had barbells and 51 walls had rectangular cross-sections. Wall web thickness ranged between 1.77 in. and 6 in. Wall aspect ratios (h_w / l_w) ranged between 0.21 and 2.0; moment-to-shear ratios (M / Vl_w) ranged between 0.25 and 2.13. The maximum aspect ratio in the barbell and flanged wall datasets are 0.63 and 1.02, respectively. Sixty-five walls were tested with applied axial load ranging between 0.022 Af_c' and 0.273 Af_c' where A is total wall area and f_c' is concrete compressive strength. Concrete compressive strength, based on standard cylindrical tests, varied between 2370 and 8463 psi. Eight walls did not have vertical web reinforcement, 6 walls did not have horizontal web reinforcement and 3 walls did not have any web reinforcement. Ninety-two of the 100 walls that had vertical and horizontal web reinforcement had two curtains of web reinforcement. Eleven of the 111 test specimens did not comply with the minimum reinforcement requirements ($\rho_h = \rho_v = 0.25\%$) of ACI 318-08 [ACI (2008)] for *Special Structural Walls and Concrete Beams* (Chapter 21.9). The maximum observed horizontal and vertical reinforcement ratios were 2.80%. Eighty-nine of the 111 test specimens were tested using cyclic loading, 21 were tested using monotonic loading and one was tested using an earthquake simulator. Wall scales in the dataset ranged between 0.22 and 0.75.

3 Demand Parameter Selection

The experimental data described in Section 2 was mined to prepare fragility curves. The fragility curves are presented as a function of racking drift, which is the best single story-level demand parameter for most structural elements such as walls. Importantly, drift is the demand parameter most reported in the literature.

Two other demand parameters were considered for this study but were set aside. Dissipated hysteretic energy [Park and Ang (1985)] has been used to assess damage to concrete components. However, the literature rarely includes hysteretic loops that are amenable to digitization and calculation of dissipated energy and so this demand parameter cannot be computed with high confidence. Pagni and Lowes (2006) and Brown and Lowes (2007) proposed a variant on dissipated hysteretic energy for assessment of reinforced concrete beam-column joints, namely, a demand parameter whose functional form included maximum story drift and number of load (or displacement) cycles as variables. Unfortunately, many sources did not report the relationship between damage and number of loading cycles and the Lowes demand parameter was not pursued.

4 Damage States and Methods of Repair

Damage states (DS) define threshold levels of damage sustained by structural components under earthquake loading. A family of damage states, which are listed in Table 7, was assembled following analysis of test data and review of the literature. Damage states are characterized generally by direct indicators of damage such as initiation of cracking, maximum concrete crack width, extent of concrete crushing, sliding shear displacement, and

reinforcement yielding, buckling, and fracture. Each of these damage states is linked with one of four methods of repair in the table.

Documents that provide guidelines for repair of reinforced concrete walls (e.g., FEMA 306 [ATC (1998b)] and FEMA 308 [ATC (1998a)]), repair of concrete (e.g., ACI 546R-04 [ACI (2004)]), observations from experimental programs, previous research on retrofit of squat walls and the expert opinion of the authors and other members of the ATC-58 Project Team (Messrs. Hamburger, Heintz and Bachman, Drs. Hanson and Kennedy, and Professors Mahin and Ellingwood) were used to identify the most appropriate damage states and their corresponding methods of repair. The following subsections present information on each Method of Repair (MoR) and the corresponding damage states. The number of damage data obtained for each wall and method of repair is presented in Table 1, Table 3, and Table 5, for rectangular, barbell and flanged walls, respectively. Appendix A presents all of the damage data analyzed in the body of the report.

4.1 MoR-1, Cosmetic Repair

Damage states DS1.1 through DS1.4 of Table 7 are associated with cosmetic repair. These damage states represent the initiation of cracking in concrete and initial propagation of these cracks under earthquake loading. For cosmetic repair, crack widths are small (less than 0.02 in. as defined in DS1.4) and structural repair to restore strength and stiffness is unnecessary. Repair of the surface finishes may be required to restore the aesthetic appearance, maintain fire resistance and prevent water infiltration into the wall [ATC (1998a)].

Cosmetic repair has no impact on structural performance. Method of Repair MoR-1 is similar to Cosmetic Repair 1 (CR1) of FEMA 308. Examples of damage states 1.2 and 1.3, each of which is linked to MoR-1, are presented in Figure 1 and Figure 2.

ID	Damage States	Method of Repair (MoR)
DS1.1	Initiation of cracking	Cosmetic repair (MoR-1)
DS1.2	Initiation of flexural cracking	
DS1.3	Initiation of shear cracking	
DS1.4	Maximum measured crack widths less than 0.02 in. (0.5 mm)	
DS2.1	Initiation of yielding in horizontal web reinforcement	Epoxy injection (MoR-2)
DS2.2	Initiation of yielding in vertical web reinforcement	
DS2.3	Initiation of yielding in vertical boundary element reinforcement	
DS2.4a	Maximum measured shear crack widths larger than 0.02 in (0.5 mm) but less than 0.12 in. (3 mm)	
DS2.5a	Maximum measured flexural crack widths larger than 0.02 in (0.5 mm) but less than 0.12 in. (3 mm)	
DS2.4b	Maximum measured shear crack widths larger than 0.04 in (1.0 mm) but less than 0.12 in. (3 mm)	
DS2.5b	Maximum measured flexural crack widths larger than 0.04 in (1.0 mm) but less than 0.12 in. (3 mm)	
DS3.1	Concrete crushing at the compression toes / initiation of crushing in the wall web	Partial wall replacement (MoR-3)
DS3.2	Vertical cracking in the toe regions of the web	
DS3.3	Buckling of boundary element vertical reinforcement	
DS3.4	Flexural crack widths exceeding 0.12 in. (3 mm)	
DS4.1	Initiation of sliding	Wall replacement (MoR-4)
DS4.2	Wide diagonal cracks	
DS4.3	Widespread crushing of concrete	
DS4.4	Reinforcement fracture	
DS4.5	Shear crack widths exceeding 0.12 in (3 mm)	

Table 7 Damage states and corresponding methods of repairs

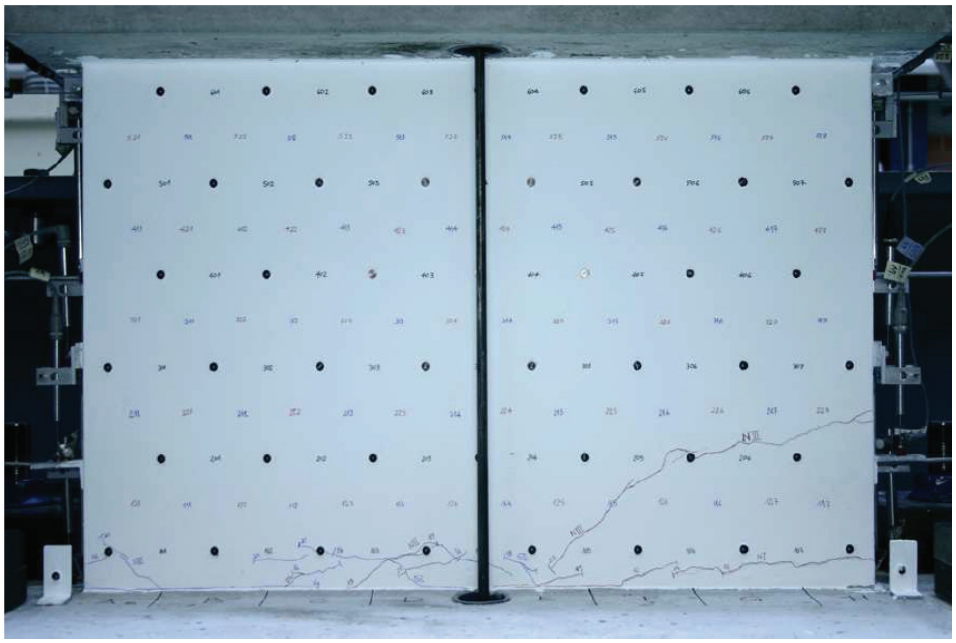

Figure 1 Initial flexural cracks on wall M4 tested by Greifenhagen et al. (2005)

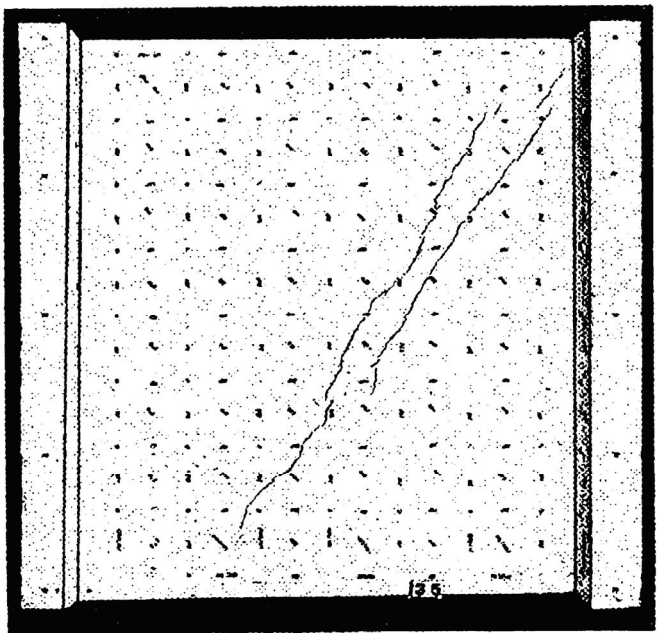

Figure 2 Initial shear cracks on wall S2 tested by Maier and Thürlimann (1985)

4.2 MoR-2, Epoxy Injection

4.2.1 Introduction

Damage states DS2.1, DS2.2, DS2.3, DS2.4a, DS2.5a, DS2.4b and DS2.5b of Table 7 are associated with epoxy-injection repair. Epoxy injection is widely used to restore the stiffness

and strength of cracked concrete components. Crack width (DS2.4a, DS2.5a, DS2.4b and DS2.5b) and reinforcement yielding (DS2.1, DS2.2 and DS2.3) are considered two indicators of the need for epoxy injection repair.

Method of Repair MoR-2 is similar to Structural Repair 1 of FEMA 308. Examples of damage states DS2.1, DS2.3 and DS2.4a, each of which is linked to MoR-2, are presented in Figure 3, Figure 4 and Figure 5, respectively. There is no consensus in the design professional community on the minimum residual crack width for epoxy injection. Herein, we present two options for consideration, MoR-2a and MoR-2b, which are described below.

4.2.2 MoR-2a

Lowes and Li (2008) note that residual crack widths in excess of 0.01 to 0.02 in. require epoxy injection to restore component strength and stiffness. However, residual crack widths are not reported in the literature and could therefore not be used to identify the need for injecton grouting. Rather, maximum crack width, which is presented in the literature, is used as a surrogate for residual crack width: if the reported maximum crack width under loading exceeds 0.02 in (0.5 mm), (assumed equivalent to DS2.4a and DS2.5a in Table 7) epoxy injection is required. Reinforcement yielding (DS2.1, DS2.2 and DS2.3) was used as another indicator for epoxy injection, on the basis that reinforcement yielding will result in residual cracks of substantial width. This relationship is studied in Section 6.

4.2.3 MoR-2b

Method of Repair MoR-2b involves injection grouting of cracks for which the maximum crack width under loading exceeds 0.04 (1.0 mm), that is DS2.4b and DS2.5b in Table 7.

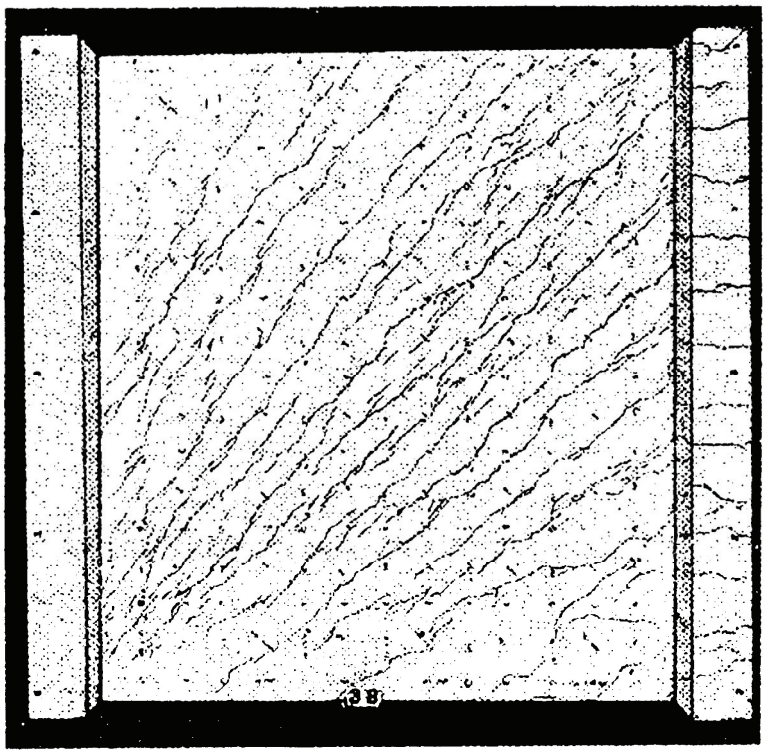

Figure 3 Cracking pattern for wall S3 tested by Maier and Thürlimann (1985) at first yielding of horizontal web reinforcement

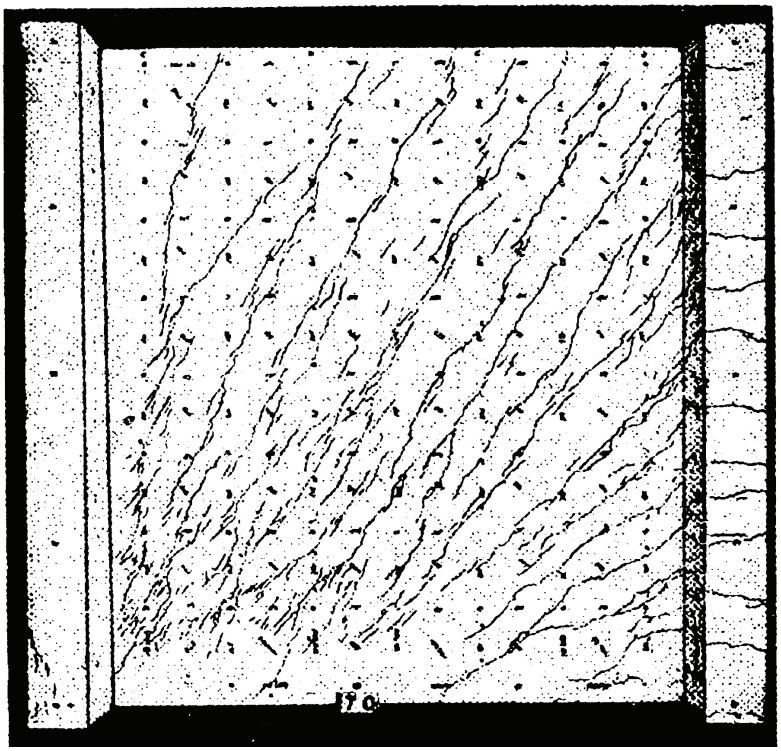

Figure 4 Cracking pattern for wall S2 tested by Maier and Thürlimann (1985) at first yielding of flange vertical reinforcement

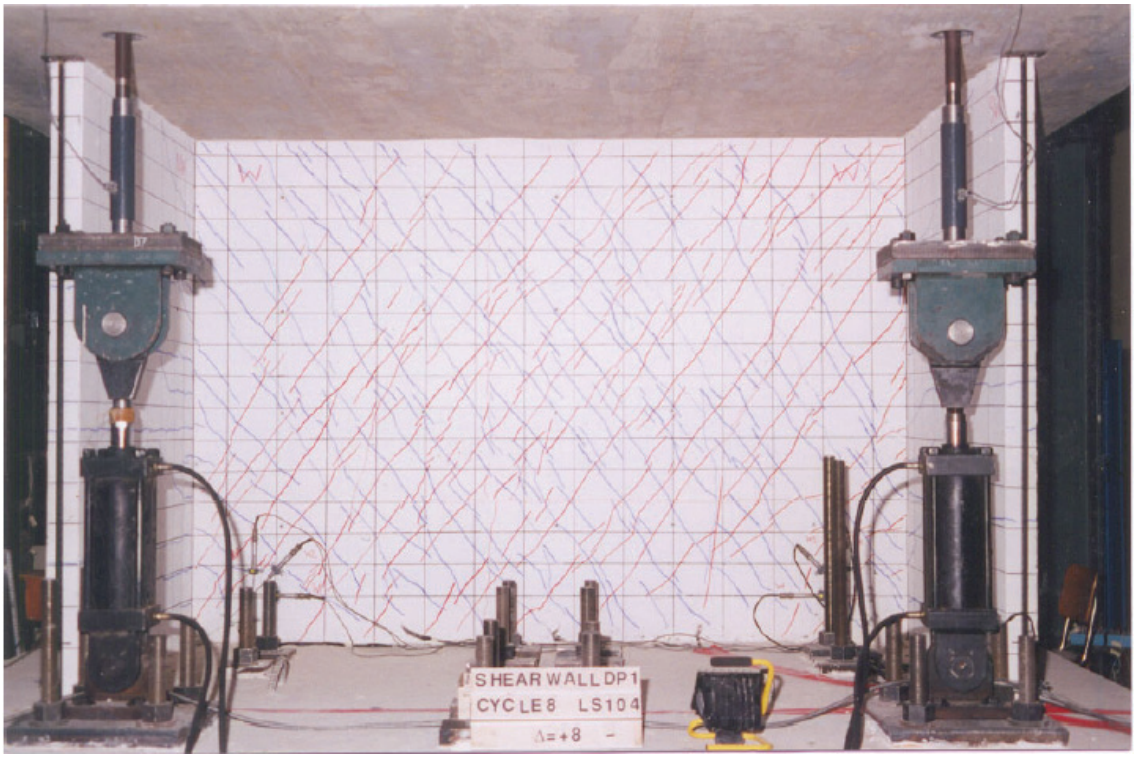

Figure 5 Cracking pattern for wall DP1 tested by Palermo and Vecchio (2002) at a maximum shear crack width of 0.5 mm

4.3 MoR-3, Partial Wall Replacement

Damage states DS3.1 through DS3.4 of Table 7 are associated with removal and replacement of damaged concrete. Localized crushing at boundary elements and in the wall web will require replacement of damaged concrete. Vertical splitting cracks in boundary elements (DS3.2) and buckling of boundary element vertical reinforcement (DS3.3) are also linked to this MoR. Photographs of test specimens and observations made by the cited authors were used to identify data for damage states DS3.1, DS3.2 and DS3.3. Damage state DS3.4 assumes that a wall with flexural crack widths greater than 0.12 in. (3 mm) cannot be repaired to its pre-earthquake condition using epoxy injection and that damaged concrete and rebar must be replaced. Examples of damage states DS3.1 and DS3.4 are presented in Figure 6 and Figure 7, respectively.

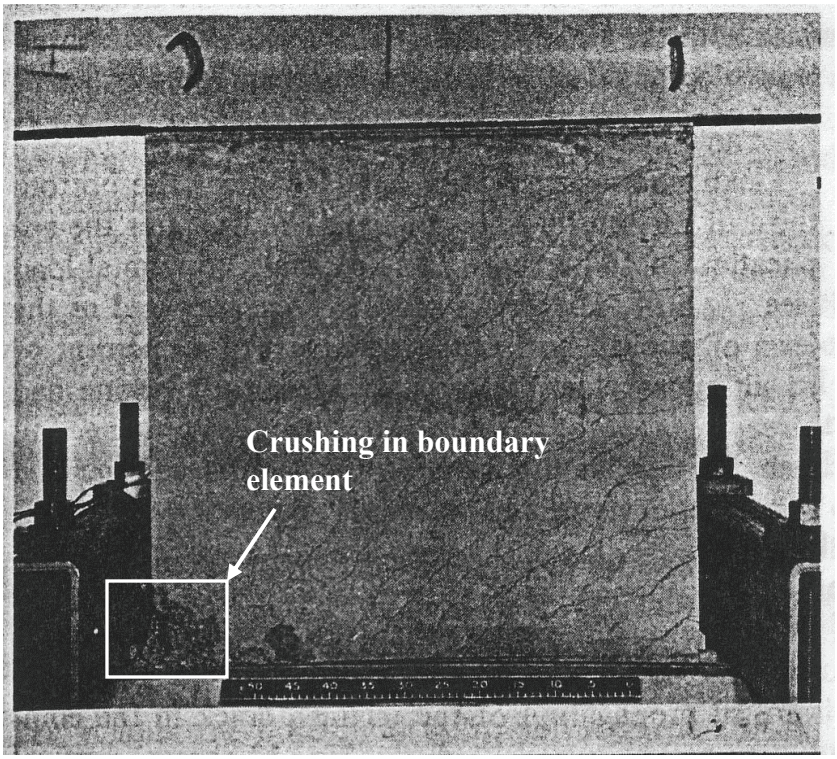

Figure 6 Cracking pattern for wall SW11 tested by Lefas et al. (1990) at compression zone failure

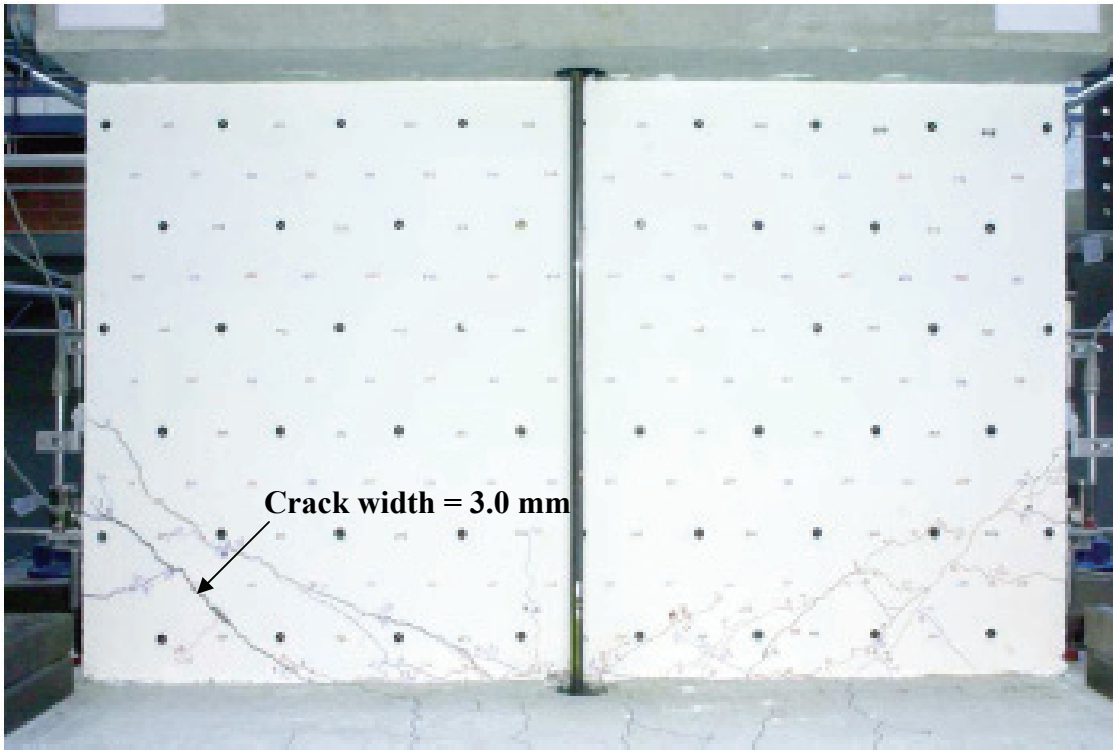

Figure 7 Cracking pattern for wall M2 tested by Greifenhagen et al. (2005) at a maximum flexural crack width of 3.0 mm

4.4 MoR-4, Wall Replacement

Damage states DS4.1 through DS4.5 of Table 7 are associated with complete replacement of the wall panel.

Sliding at the interface between the wall web and the foundation (DS4.1) will require wall panel replacement, especially if the residual displacement is significant. Squat walls with low vertical reinforcement ratio and low axial load are susceptible to sliding shear. A cracking pattern for damage state DS4.1 is presented in Figure 8. Substantial corner-to-corner diagonal cracks (DS 4.2) which are indicators of diagonal tension (DT) or flexure-diagonal tension (F-DT) failures [Gulec (2009)], trigger rapid loss in strength and stiffness. Such walls cannot be repaired using epoxy injection because the crack widths are too great and partial wall replacement is not feasible because of the orientation and length of the cracks. Squat walls with light horizontal reinforcement are susceptible to this type of damage. Figure 9 presents a cracking pattern for damage state DS4.2.

Walls with heavy reinforcement and/or high axial loads usually fail in diagonal compression (crushing of compression struts) as shown in Figure 10. The damage is so widespread that partial wall replacement is not feasible and the entire wall panel must be replaced (DS4.3). Reinforcement fracture (DS4.4) is rarely seen in tests of squat walls. Reinforcement fractured in only 3 of the 100 walls. Damage state DS4.4 is linked to wall replacement because reinforcement fracture followed other significant damage in all three cases. Figure 11 shows the cracking pattern in a wall at the fracture of boundary element vertical reinforcement. Widespread damage at the interface between the wall web and foundation is evident in the figure. Damage State DS4.5 assumes that wall panels with maximum shear crack widths larger than 0.12 in (3 mm) must be replaced. FEMA 306 [ATC (1998b)] notes that when the

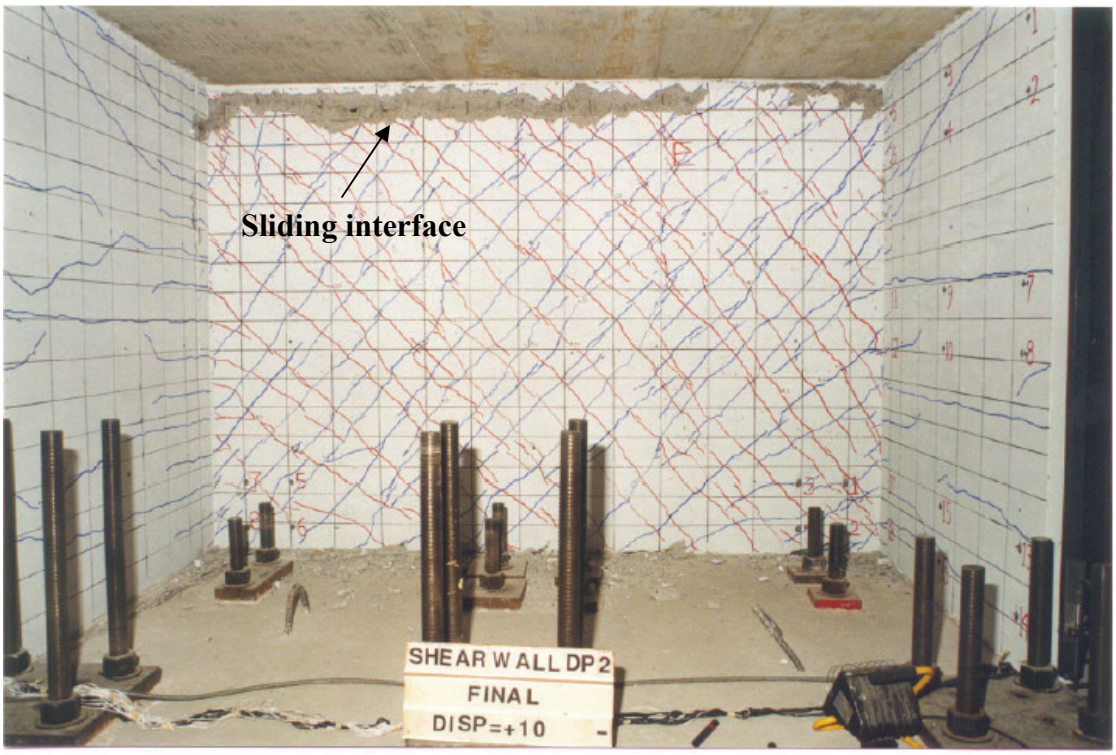

Figure 8 Cracking pattern for wall DP2 tested by Palermo and Vecchio (2002) at a sliding failure between the wall web and top slab

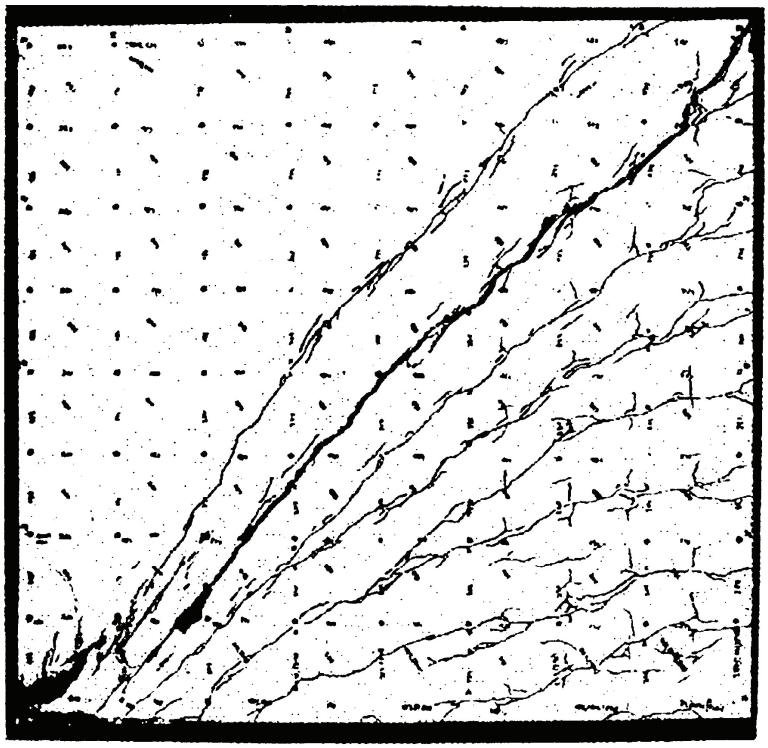

Figure 9 Cracking pattern for wall S9 tested by Maier and Thürlimann (1985) at diagonal tension failure

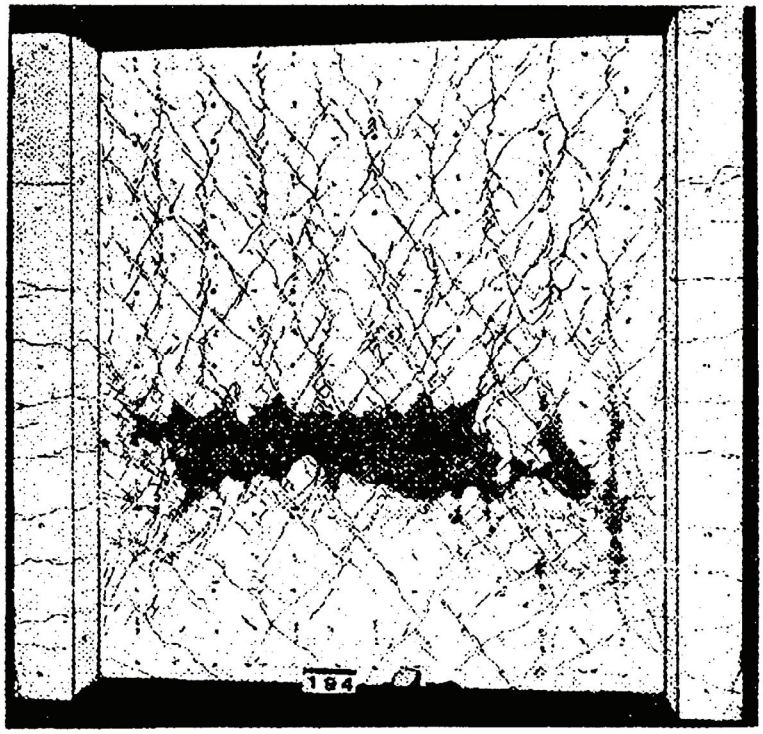

Figure 10 Cracking pattern for wall S7 tested by Maier and Thürlimann (1985) at crushing of diagonal compression struts

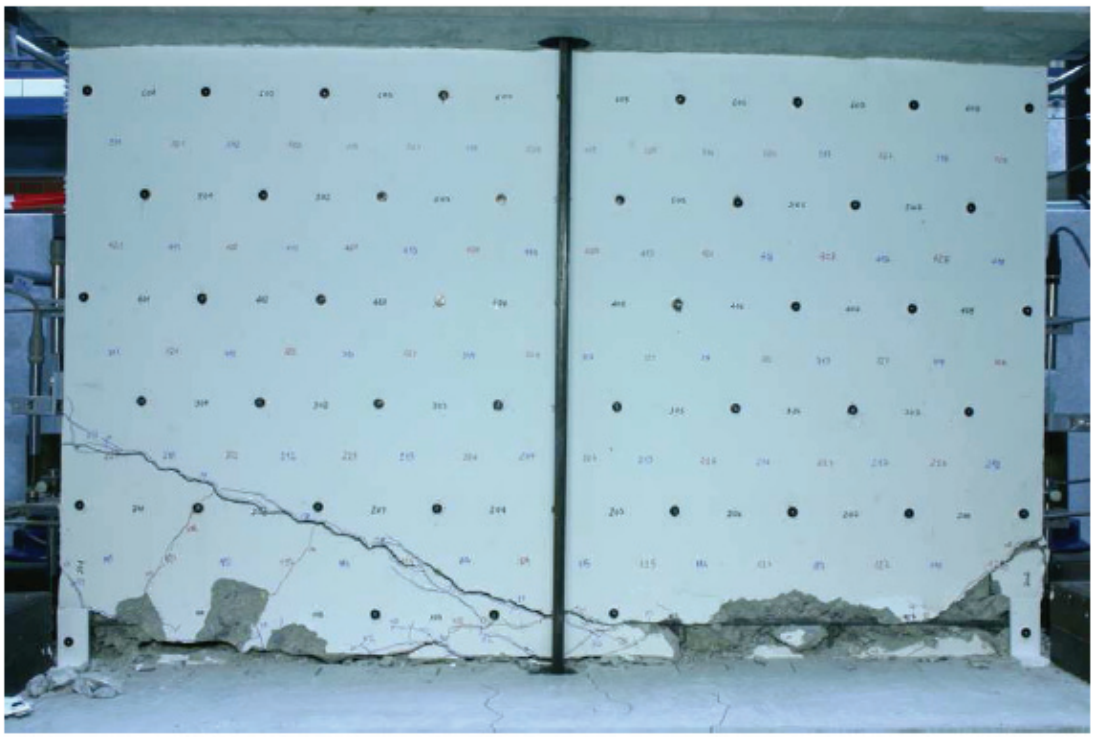

Figure 11 Cracking pattern for wall M1 tested by Greifenhagen et al. (2005) at reinforcement fracture

width of shear cracks in a wall exceed 1/8 in. (3.2 mm), the damage is considered *heavy* and restoration of the pre-earthquake strength and stiffness requires replacement of the wall. This damage state is similar to damage state DS4.2 in the sense that it is also closely related to diagonal tension (DT) and flexure-diagonal tension (F-DT) failures observed in squat walls.

The available images of damage together with the author's descriptions of damage were used wherever possible to identify the drift associated with wall replacement. A major challenge was the identification of drift corresponding to sliding shear failure (DS4.1). The author-reported drifts for sliding shear failures exhibited significant variance, for example, in some cases the authors reported the drifts at initiation of sliding whereas in others the author-reported drifts corresponding to significant sliding displacements. Two supplemental criteria are therefore used herein to aid in the identification of drift for DS4.1: 1) residual drift exceeding 0.5% (SC_1), and 2) drift associated with wall strength less than 50% of the peak strength (SC_2). Each criterion is described in more detail below. For a wall reported to have failed by sliding shear, the drift is calculated using SC_1. If a drift cannot be computed using SC_1, SC_2 is used. If a drift cannot be computed using SC_2, no data is reported for DS4.1. *Supplemental Criterion* SC_1: If a cyclic force-displacement relationship was available, the peak transient drift associated with a residual drift angle of 0.5% was estimated. The residual drift angle of 0.5% was associated with a zero-force displacement intercept of 1% story drift angle. Given that the coda portion of earthquake ground motions will generally serve to partially re-center displaced components, elements and building frames, we assumed that a residual drift angle of 1% from a displacement-controlled cyclic test would be reduced to 0.5% in an earthquake. Only first cycle curves at each displacement level were considered for computation of the drifts at which the drifts at zero-load exceed 1.0%.To illustrate this

computation, consider Figure 12 that presents the load-displacement data for wall M1 reported in Greifenhagen et al. (2005). In the figure, the peak transient drifts in the first (1.47%) and third quadrants (2.70%) for which the residual drifts exceed 1.0% are identified using red circles. The smaller of the two drifts is assumed to mark the onset of sliding shear failure and used for further analysis.

Supplemental Criterion SC_2: A backbone load-displacement relationship for the first and third quadrants is prepared using the first cycle shear strengths at each displacement increment. The peak resistance of the wall is computed as the maximum force in the first and third quadrants. The story drifts in the first and third quadrants at which the resistance dropped below 50% of the peak resistance are calculated and the smaller of the two story drifts is chosen for further analysis. The computation is illustrated in Figure 13 in which backbone force-displacement curves are presented in the first and third quadrants. The peak shear strengths of the wall (in the first quadrant in this case) and the drifts at a post-capping shear strength equal to 50% of the peak resistance in the first quadrant and third quadrants, equal to 3.84% and -3.47%, respectively, are identified in the figure.

The supplemental criteria are used primarily to identify transient drifts associated with sliding shear failures but are also used if a failure by either diagonal tension or compression is reported but the drift at failure is not, the drift associated with SC_2 is reported.

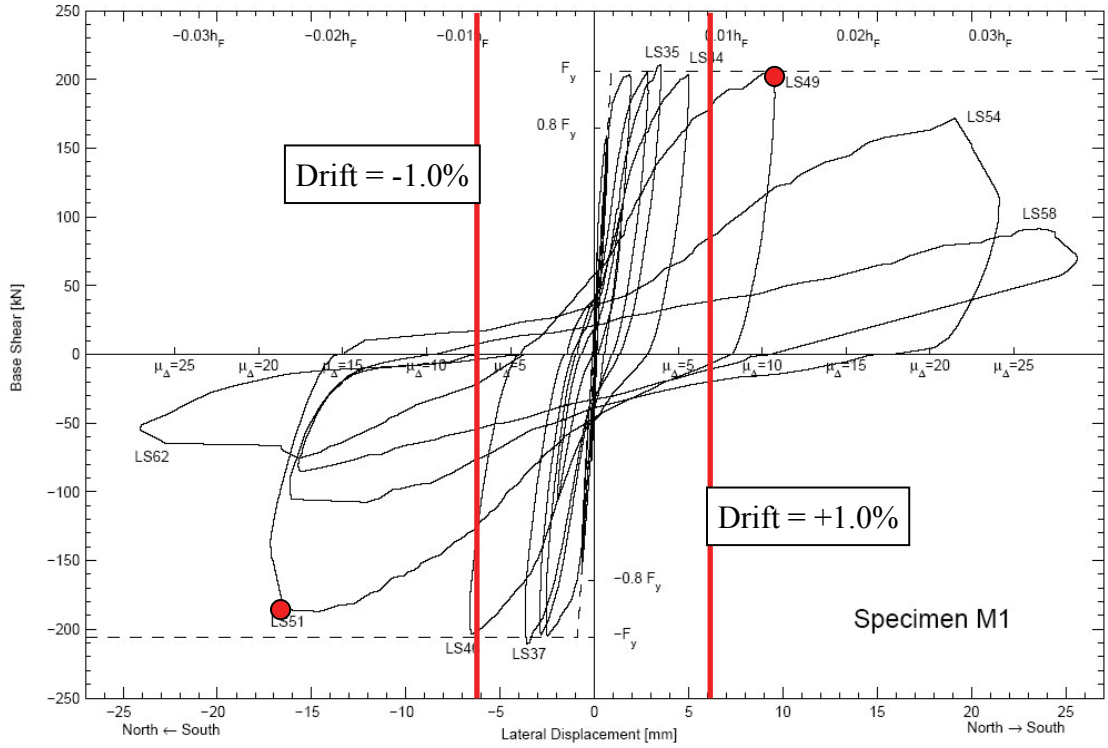

Figure 12 Residual drift computation on the force-drift relationship for M1 tested by Greifenhagen et al. (2005)

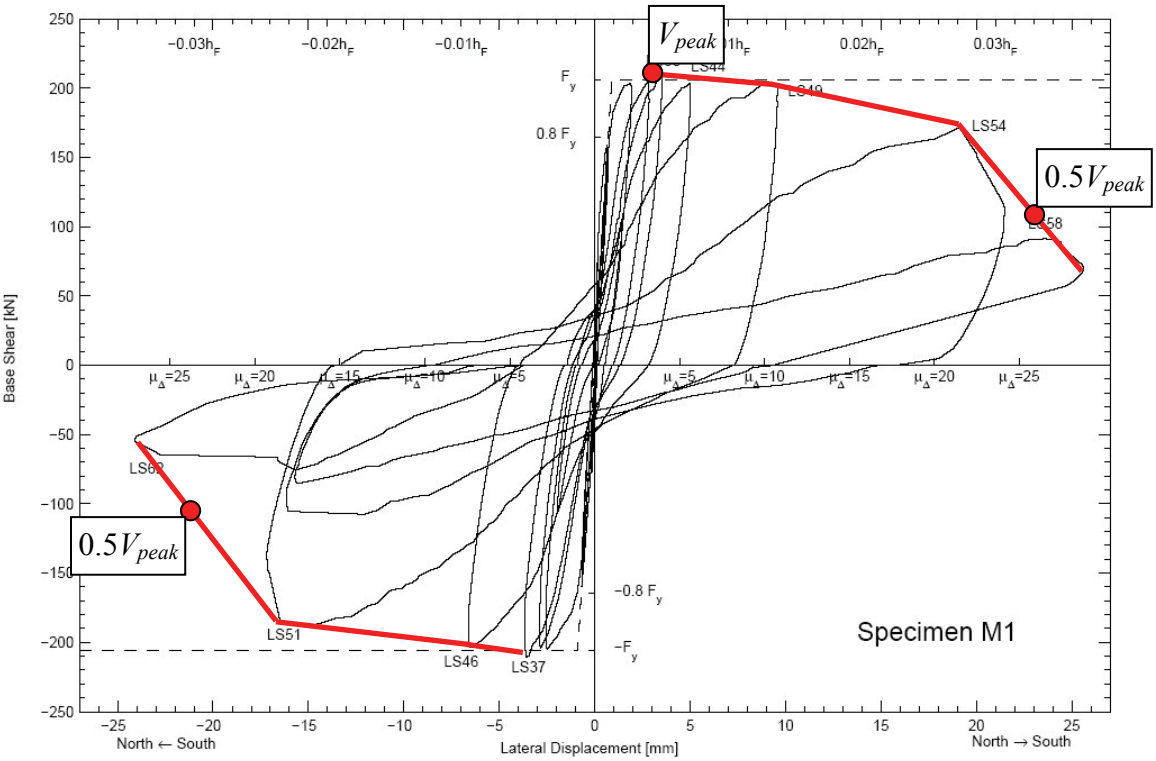

Figure 13 Determination of drifts at which the force-peak shear strength drops to 50% of the peak for M1 tested by Greifenhagen et al. (2005)

5 Fragility Analysis

5.1 Introduction

Herein, fragility functions are developed to characterize the probability that a specific MoR will be required as a function of racking (shear) drift. Data from tests of 111 walls (see Section 2) are analyzed. Damage states (or methods of repair) are presented using continuous probability distributions. The method of maximum likelihood is used to fit the data. Four continuous probability distributions are considered, namely: lognormal, gamma, Weibull and beta. Empirical cumulative distribution functions are presented below together with the fitted distributions.

5.2 Characterization of Damage Data

Careful mining of damage data is essential because data for more than one damage state was identified for a given method of repair in many of the walls.

Two methods were considered to capture data for the purpose of developing fragility curves:

> **Method 1**: Data for all damage states is used, resulting in multiple data points per specimen for a given MoR.
>
> **Method 2**: Each MoR is represented by a single data point that corresponds to the damage state with the smallest drift value for a given specimen.

Figure 14 illustrates the application of the two methods. In this figure, MoR-N is any method of repair, and DSN.1 through DSN.5 are the available damage data for MoR-N.

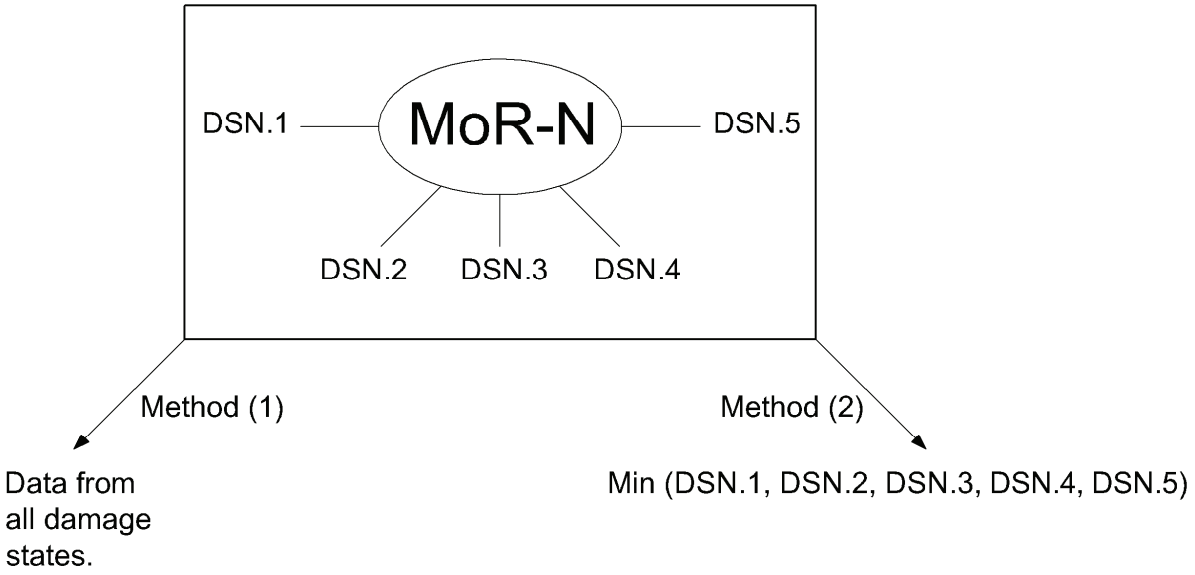

Figure 14 Schematic representation of data characterization

Using all available demand parameter-damage state pairs to create fragility curves will yield the greatest number of data points for each MoR (a maximum of 5 pairs per Figure 6-12). However, in most cases, the use of Method 1 will result in a higher mean value for a fragility function than that of Method 2 (one value per Figure 14). Fragility curves were developed using both methods to investigate the impact of the choice of data representation. Means and standard deviations for the drift data obtained using the two methods are presented in Table 8 for each MoR; data are presented for both MoR-2a and MoR-2b. As seen in the table, the means calculated using Method 1 are higher than those calculated using Method 2. Variability, as measured by coefficient of variation, is higher for Method 1 except for MoR-3. The impact of the choice of method is more significant for MoR-1 and MoR-2a because, in many cases, two or more values of drift could be associated with these methods of repair for a given wall. In most instances, a single drift could be identified for each wall for MoR-2b, MoR-3 and MoR-4.

MoR	Method 1			Method 2		
	Mean	Standard deviation	Coeff. of Variation	Mean	Standard deviation	Coeff. of Variation
1	0.12	0.14	1.20	0.07	0.09	1.20
2a	0.50	0.28	0.55	0.42	0.18	0.44
2b	0.62	0.22	0.36	0.62	0.23	0.37
3	0.84	0.39	0.46	0.83	0.41	0.50
4	1.23	0.51	0.42	1.19	0.47	0.39

Table 8 Statistical summary of the drifts (all cross-sections) obtained using two methods for data mining for each MoR

5.3 Probability Distributions

Four probability distributions that are widely used for engineering applications, namely, lognormal, gamma, Weibull and beta, were used to fit the compiled damage data. All four distributions require positive values of the random variable (demand parameter). Figure 15 presents sample probability density functions for the four distributions. The following subsections present summary information on these probability distributions. The variable x is used to represent the random variable (= story drift).

5.3.1 Lognormal Distribution

The lognormal distribution is a one-sided probability distribution of a random variable whose logarithm is normally distributed. This distribution is widely used for fragility studies because the demand parameter (drift or acceleration) must be positive and its relationship with the normal or Gaussian distribution. Equation 1 presents the probability density function (pdf) for the lognormal distribution.

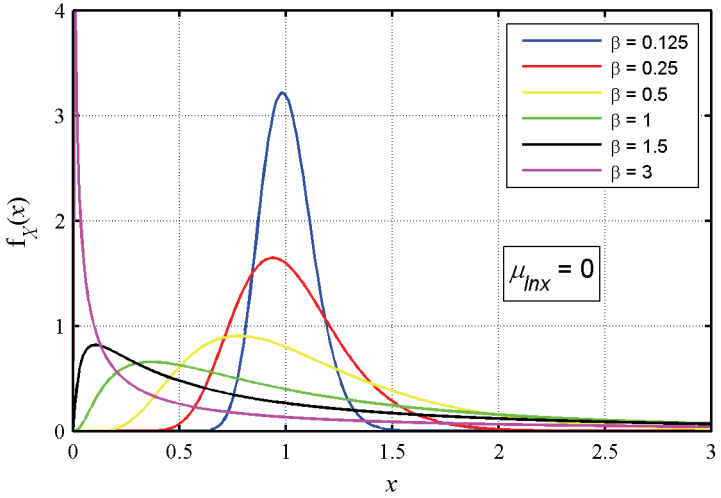

a) lognormal distribution

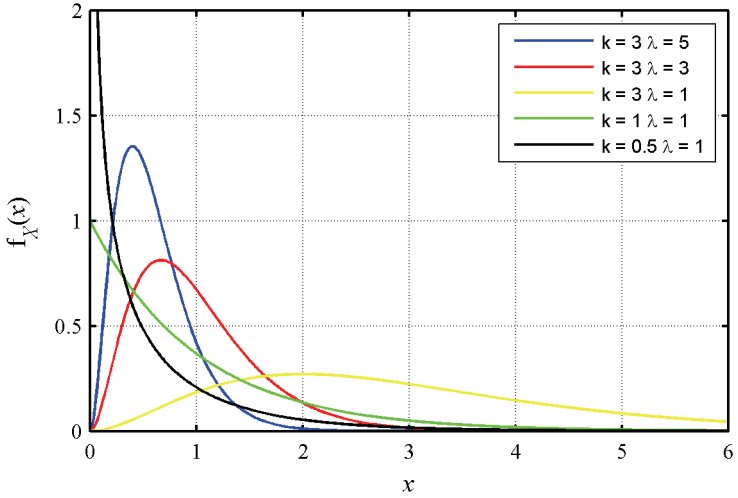

b) gamma distribution

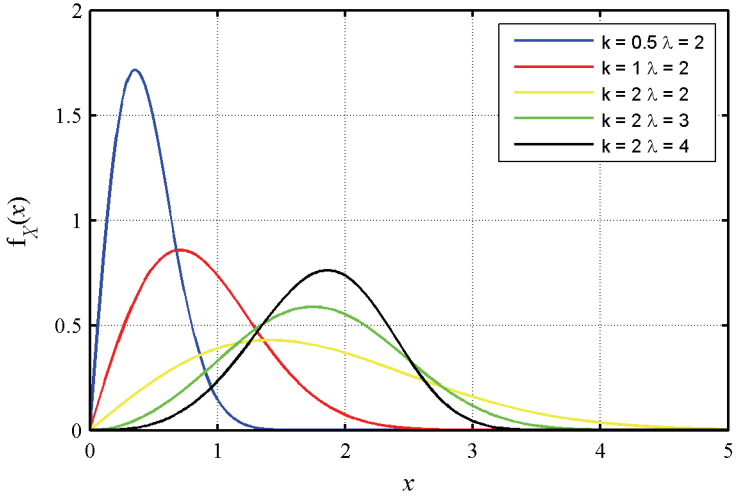

c) Weibull distribution

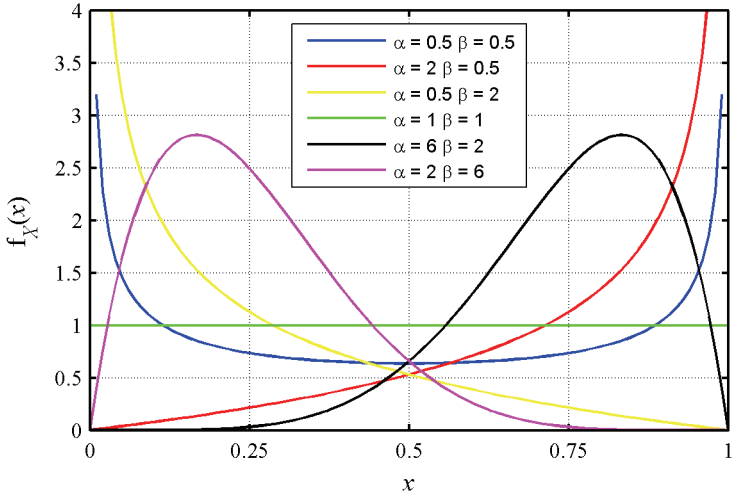

d) beta distribution

Figure 15 Families of probability density functions for the four distributions utilized herein

$$f_X(x) = \begin{cases} \dfrac{1}{x\sigma_{\ln x}\sqrt{2\pi}} \exp\left[-\dfrac{\left(\ln(x) - \mu_{\ln x}\right)^2}{2\sigma_{\ln x}^2} \right] & \text{for } x \geq 0 \\ 0, \quad \text{elsewhere} \end{cases} \tag{1}$$

In Equation 1, $\mu_{\ln x}$ and $\sigma_{\ln x}$ are the mean and standard deviation of the natural logs of the demand parameter. The standard deviation of the natural log of the data, $\sigma_{\ln x}$, is termed dispersion in the ATC-58 project [ATC (2008)] and is denoted as β. The median (θ), mean (μ) and standard deviation (σ) for a lognormally distributed demand parameter (x) are presented in Equations 2 through 4.

$$\theta = \exp(\mu_{\ln x}) \tag{2}$$

$$\mu = \theta \exp\left(\frac{\sigma_{\ln x}^2}{2} \right) \tag{3}$$

$$\sigma = \mu \sqrt{\exp\left(\sigma_{\ln x}^2\right) - 1} \tag{4}$$

5.3.2 Gamma Distribution

Similar to the lognormal distribution, the gamma distribution is also one-sided. Equation 5 presents the probability density function for the gamma distribution. The gamma distribution uses two parameters, k and λ. The parameter k defines the shape of the distribution and λ is a scale parameter. The probability density function for the gamma distribution is unimodal with its peak at $x = 0$ for $k \leq 1$, and at $x = (k-1)/\lambda$ for $k > 1$ [Soong (2004)].

$$f_X(x) = \begin{cases} \dfrac{\lambda^k}{\Gamma(k)} x^{k-1} e^{-\lambda x} & \text{for } x \geq 0 \\ 0, \quad \text{elsewhere} \end{cases} \tag{5}$$

where $\Gamma(k)$ is the gamma function:

$$\Gamma(k) = \int_0^\infty u^{k-1} e^{-u} du \tag{6}$$

If k is a positive integer, the gamma function takes the form:

$$\Gamma(k) = (k-1)! \tag{7}$$

where ! denotes factorial. The mean (μ) and standard deviation (σ) for a gamma-distributed variable are:

$$\mu = \frac{k}{\lambda} \quad \text{and} \quad \sigma = \frac{\sqrt{k}}{\lambda} \tag{8}$$

5.3.3 Weibull Distribution

The Weibull distribution is an extreme value distribution of type III [Soong (2004)]. Equation 9 presents the probability density function for the Weibull distribution. Similar to the gamma distribution, k defines the shape of the distribution and λ is a scale parameter.

$$f_X(x) = \frac{k}{\lambda}\left(\frac{x}{\lambda}\right)^{k-1} \exp\left[-\left(\frac{x}{\lambda}\right)^k\right] \quad k, \lambda > 0 \quad x \geq 0 \tag{9}$$

The mean (μ) and the standard deviation (σ) for a Weibull-distributed variable are:

$$\mu = \lambda\Gamma\left(1+\frac{1}{k}\right) \quad \text{and} \quad \sigma = \lambda\sqrt{\Gamma\left(1+\frac{2}{k}\right) - \Gamma^2\left(1+\frac{1}{k}\right)} \tag{10}$$

Brown (2008) notes that the Weibull distribution is appropriate for developing fragility functions because it provides accurate results with small data sets and represents a broad range of distribution shapes, which enables easier fitting.

5.3.4 Beta Distribution

The beta distribution is a versatile distribution defined on the interval [0, 1]. The probability density function for the beta distribution is:

$$f_X(x) = \begin{cases} \dfrac{1}{B(\alpha,\beta)} x^{\alpha-1}(1-x)^{\beta-1} & \text{for } 0 \le x \le 1 \\ 0, \quad \text{elsewhere} \end{cases} \tag{11}$$

where B is the beta function as calculated using Equation 12.

$$B(\alpha,\beta) = \frac{\Gamma(\alpha)\Gamma(\beta)}{\Gamma(\alpha+\beta)} \tag{12}$$

The parameters α and β are both shape parameters that take on positive values only. When $\alpha,\beta > 1$, the density function is unimodal with the peak at $(\alpha-1)/(\alpha+\beta-2)$. The density function becomes U-shaped when $\alpha,\beta < 1$; J-shaped when $\alpha \ge 1,\ \beta < 1$; reverse J-shaped when $\alpha < 1,\ \beta \ge 1$; and uniform when $\alpha = \beta = 1$ [Soong (2004)]. The mean (μ) and standard deviation (σ) of a beta-distributed variable are:

$$\mu = \frac{\alpha}{\alpha+\beta} \quad \text{and} \quad \sigma = \frac{1}{\alpha+\beta}\sqrt{\frac{\alpha\beta}{\alpha+\beta+1}} \tag{13}$$

Since the beta distribution is defined on the interval [0, 1], experimental data must be transformed to the interval [0, 1] before fitting the distribution.

5.4 Method of Maximum Likelihood

The method of maximum likelihood is the most widely used rule for finding point estimations of distribution parameters for sample data and is used below to estimate the parameters for the aforementioned distributions. This method makes use of the sample likelihood function that is presented below for completeness.

First, let $f(x;\theta)$ be the probability density function of the population where θ is(are) the parameter(s) of the distribution X. The joint density function of a sample $X_1, X_2, \ldots, X_n$ has the form:

$$f_{X_1,X_2,\ldots,X_n}(x_1,x_2,\ldots,x_n|\theta) = f_{X_1}(x_1)f_{X_2}(x_2)\cdots f_{X_n}(x_n) = \Pi f_X(x_i|\theta) \tag{14}$$

where Π denotes product.

The *likelihood function* $L(\theta)$ of a set of *n* sample values is

$$L(\theta|x_1,x_2,\ldots x_n) = \prod_{i=1}^{n} f_X(x_i|\theta) \tag{15}$$

which gives the *relative likelihood* of having observed this particular sample ($X_1 = x_1$, $X_2 = x_2, \ldots, X_n = x_n$) as a function of θ [Benjamin and Cornell (1970)].

The *maximum likelihood estimate* (MLE) of θ is the value that maximizes the *likelihood function* $L(\theta)$. Per Benjamin and Cornell, maximum likelihood estimators possess the following desirable properties

- *Asymptotical unbiasedness*: means are asymptotically ($n \to \infty$) equal to the true parameter value(s), θ
- *Efficiency*: minimum expected squared error among all possible unbiased estimators.
- *Consistency*: be close to the true parameter values as the sample size increases with uncreasingly high probability
- *Sufficiency*: make maximum use of the information contained in the data.

5.5 Goodness-of-Fit Testing

To quantify the utility of the distributions, goodness-of-fit tests were performed on each fit. The Kolmogorov-Smirnov test (denoted hereafter as the K-S test) is a general test that is applicable to any distribution. The Lilliefores test is a special case of Kolmogorov-Smirnov test that can assess normality only.

5.5.1 Kolmogorov-Smirnov test (K-S test)

Given a set of sample values x_1, x_2, …, x_n observed from a population X, the test parameter for the K-S test (D) is calculated as:

$$D = \max_{i=1}^{n} \left\{ \left| F_X(x_i) - S_X(x_i) \right| \right\} \tag{16}$$

In Equation 16, $F_X(x_i)$ and $S_X(x_i)$ are the theoretical and empirical CDFs, respectively, calculated at the i^{th} observation. Thus, the test parameter (D) of the K-S test corresponds to the maximum of the absolute values of n (sample size) differences between the empirical CDF and the hypothesized CDF evaluated for the observed samples. The distribution of D is independent of the hypothesized distribution and is a function of n only [Benjamin and Cornell (1970)].

The null hypothesis, H_0, for the K-S test is that the population X comes from the hypothesized probability distribution. At a specified significance level (α), if D is less than or equal to D_{crit}, the null hypothesis is accepted.

$$P(D \le D_{crit}) = 1 - \alpha \tag{17}$$

Values for D_{crit} have been tabulated [e.g., Soong (2004)] as a function of the sample size (n) and significance level (α).

The advantage of the K-S test is that it is applicable to all sample sizes and uses data in unaltered form (does not require arbitrary grouping of the sample data) unlike the chi-square goodness-of-fit test. However, the K-S test is valid strictly for continuous distributions and values for D_{crit} are based on a completely specified hypothesized distribution (parameters known). This is not the case herein since the distribution parameters are unknown and must be estimated from the data. Using the K-S test with estimated distribution parameters may result in an unconservative acceptance of the null hypothesis [Benjamin and Cornell (1970)]. Herein, the K-S test is used to evaluate the quality of the fit of the distributions relative to one another.

5.5.2 Lilliefors test

The Lilliefors test evaluates the normality of a given data. Herein, the test is used to assess the acceptability of the lognormal distribution by testing the logarithm of the available data. This test is a variant of the K-S test to account for computation of the distribution parameters from the sample data [Lilliefors (1967)]. The test statistic for the Lilliefors test is calculated in a similar manner to that for the K-S test; the difference is in the calculation of D_{crit}. The Lilliefors test accounts for the unknown sample mean and variance and uses Monte Carlo simulation to determine approximate values of D_{crit}. The Lilliefors test is valid for small sample sizes but is also appropriate when the distribution parameters are unknown [Lilliefors (1967)], which is the case in this study.

5.6 Parameters That Effect the Earthquake Performance of Low Aspect Ratio Walls

Gulec (2009) presents a detailed discussion of the failure modes for low aspect ratio reinforced concrete walls. Wall geometry, aspect ratio, horizontal web reinforcement ratio,

vertical web reinforcement ratio, and axial load were identified as the five key parameters that affect the earthquake response of squat reinforced concrete walls. Walls with boundary elements are more susceptible to diagonal compression failure than rectangular walls. As aspect ratio increases, the likelihood of developing wall flexural strength increases and the likelihood of shear failure decreases. Flexural and shear failures exhibit different damage patterns. Horizontal reinforcement is effective in resisting diagonal tension failure, and shear crack width is affected by horizontal web reinforcement ratio. Vertical web reinforcement is effective in resisting the opening of diagonal cracks and helps to anchor compression struts that transfer lateral forces to the wall foundation. Higher axial force delays diagonal tension cracking but can trigger diagonal compression failure. The effect of these five parameters on the damage data is investigated below. For completeness, two other parameters are studied: 1) wall thickness, and 2) number of curtains of web reinforcement.

Table 9 and Table 10, present a statistical summary of drifts for each MoR obtained using Methods 1 and 2, respectively, with respect to wall geometry. Results are presented to two decimal digits. In these tables, means ($\bar{x}$), standard deviations (sd), and coefficient of variation (cv) are calculated as follows

$$\bar{x} = \frac{1}{n}\sum_{i=1}^{n} x_i \quad , \quad sd = \left[\frac{1}{n-1}\sum_{i=1}^{n}\left(x_i - \bar{x}\right)^2\right]^{1/2} \quad , \quad cv = sd / \bar{x} \tag{18}$$

where n is the number of samples of x_i. The drift values obtained for walls with barbell cross sections are generally much lower than those for walls with rectangular and flanged cross sections. Note that the mean drifts for MoR-3 are smaller than MoR-2 for walls with barbell cross sections, which is attributed to the dataset used to generate damage data for barbell walls that includes many walls with low-aspect ratios and high vertical and horizontal web

reinforcement ratios (see Table 3 and Table 4). Given the results of Table 9 and Table 10 and the ranges of data presented in Table 1 through Table 6, families of fragility functions are presented for each geometry of wall.

MoR	Wall geometry								
	Rectangular			Barbell			Flanged		
	$\bar{x}$	*sd*	*cv*	$\bar{x}$	*sd*	*cv*	$\bar{x}$	*sd*	*cv*
1	0.17	0.16	0.95	0.04	0.02	0.57	0.13	0.16	1.24
2a	0.47	0.19	0.40	0.43	0.20	0.46	0.59	0.38	0.64
2b	0.58	0.20	0.34	N/A[1]	N/A	N/A	0.75	0.27	0.37
3	1.07	0.29	0.27	0.35	0.16	0.46	0.80	0.33	0.42
4	1.39	0.51	0.36	0.88	0.14	0.16	1.45	0.63	0.43

1. There is one data point for MoR-2b and barbell walls.

Table 9 Statistical summary of drifts for each MoR and Method 1

MoR	Wall geometry								
	Rectangular			Barbell			Flanged		
	$\bar{x}$	*sd*	*cv*	$\bar{x}$	*sd*	*cv*	$\bar{x}$	*sd*	*cv*
1	0.11	0.11	1.06	0.03	0.01	0.33	0.06	0.05	0.86
2a	0.43	0.15	0.36	0.38	0.19	0.50	0.42	0.22	0.53
2b	0.58	0.20	0.34	N/A[1]	N/A	N/A	0.77	0.30	0.39
3	1.10	0.31	0.29	0.35	0.16	0.46	0.80	0.34	0.43
4	1.32	0.42	0.32	0.88	0.14	0.16	1.45	0.63	0.43

1. There is one data point for MoR-2b and barbell walls.

Table 10 Statistical summary of drifts for each MoR and Method 2

Figure 16 presents the variation of drift with aspect ratio for MoR-1, MoR-2a, MoR-3 and MoR-4. All available damage data are included in the figure (and in Figure 17, Figure 18, and Figure 19). For barbell and flanged walls, no trends are evident for any of the MoRs considered. For walls with rectangular cross-sections, there is a weak trend of increasing drift with increasing aspect ratio for MoR-1. However, scatter is significant and the size of the

rectangular wall dataset for MoR-1 for aspect ratios of between 1.0 and 2.0 is small, with most of the data clustered around 2.0. In summary, the available data do not reveal any strong correlation between aspect ratio and damage for any wall geometry.

Figure 17 presents the variation of drift with horizontal web reinforcement ratio for each method of repair. No relationship between drift and horizontal web reinforcement ratio can be identified for any method of repair for either rectangular or flanged walls. The limiting drifts for MoR-1, MoR-3 and MoR-4 for barbell walls are independent of horizontal web reinforcement ratio. A weak trend of increasing drift with increasing horizontal web reinforcement ratio is seen for MoR-2a but the scatter is quite large and sample size is modest.

Figure 18 presents the variation of drift with vertical web reinforcement ratio for each method of repair. No visible trends between drift and vertical web reinforcement ratio are evident for any method of repair for rectangular and flanged walls. For the barbell walls, the limiting drifts for MoR-1, MoR-3 and MoR-4 are independent of vertical web reinforcement ratio. For MoR-2a, a trend of increasing drift with increasing vertical web reinforcement ratio is evident. Note that all barbell walls considered herein had equal percentages of horizontal and vertical web reinforcement and that the trends observed with drift and vertical web reinforcement ratio for barbell walls for all methods of repair are similar to those observed with drift and horizontal web reinforcement ratio.

Figure 19 presents the variation of drift with normalized axial load for each method of repair. No significant trends between drift and normalized axial load are evident for any method of repair for any cross-section type. However, the number of data for normalized axial loads of higher than 10% is very small as seen in Figure 19.

The variation of drift with wall web thickness for each method of repair is presented in Figure 20. No significant trends between drift and wall web thickness are evident for any method of repair for any cross-section type except for MoR-1 and rectangular walls.

Figure 21 presents the variation of drift with number of curtains of orthogonal web reinforcement for each method of repair. Since the number of damage data for walls with a single curtain of orthogonal web reinforcement is small, the effect of number of curtains of web reinforcement on damage data cannot be established statistically. A visual interpretation of the data indicates that story drift is smaller for MoR-1, MoR-2a and MoR-4 for a single curtain of reinforcement. More experimental data is needed to investigate this relationship further.

In summary, the available data do not support the use of aspect ratio, horizontal and vertical web reinforcement ratio, axial load, web thickness and number of web reinforcement curtains as variables in the presentation of fragility curves. Although horizontal and vertical web reinforcement ratios have an impact on the limiting drifts for MoR-2a, the dispersion is substantial. Only wall geometry substantially influences the relationships. The barbell wall dataset yielded significantly different damage characteristics than walls with flanged and rectangular walls as presented in Table 9 and Table 10. Although the damage data for rectangular and flanged walls are comparable, the ranges on the two datasets are significantly different.

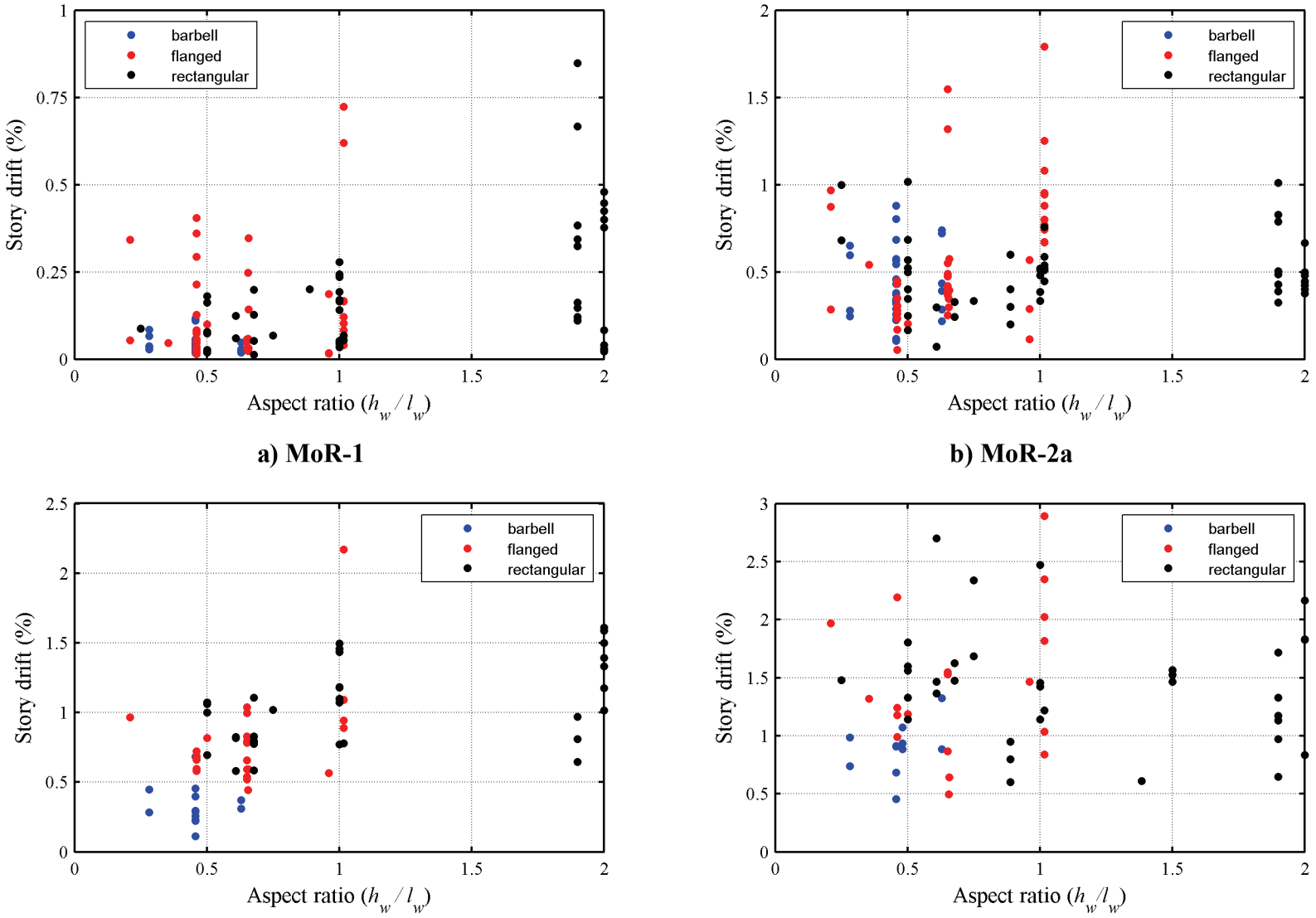

Figure 16 Variation of drift with aspect ratio for different methods of repair

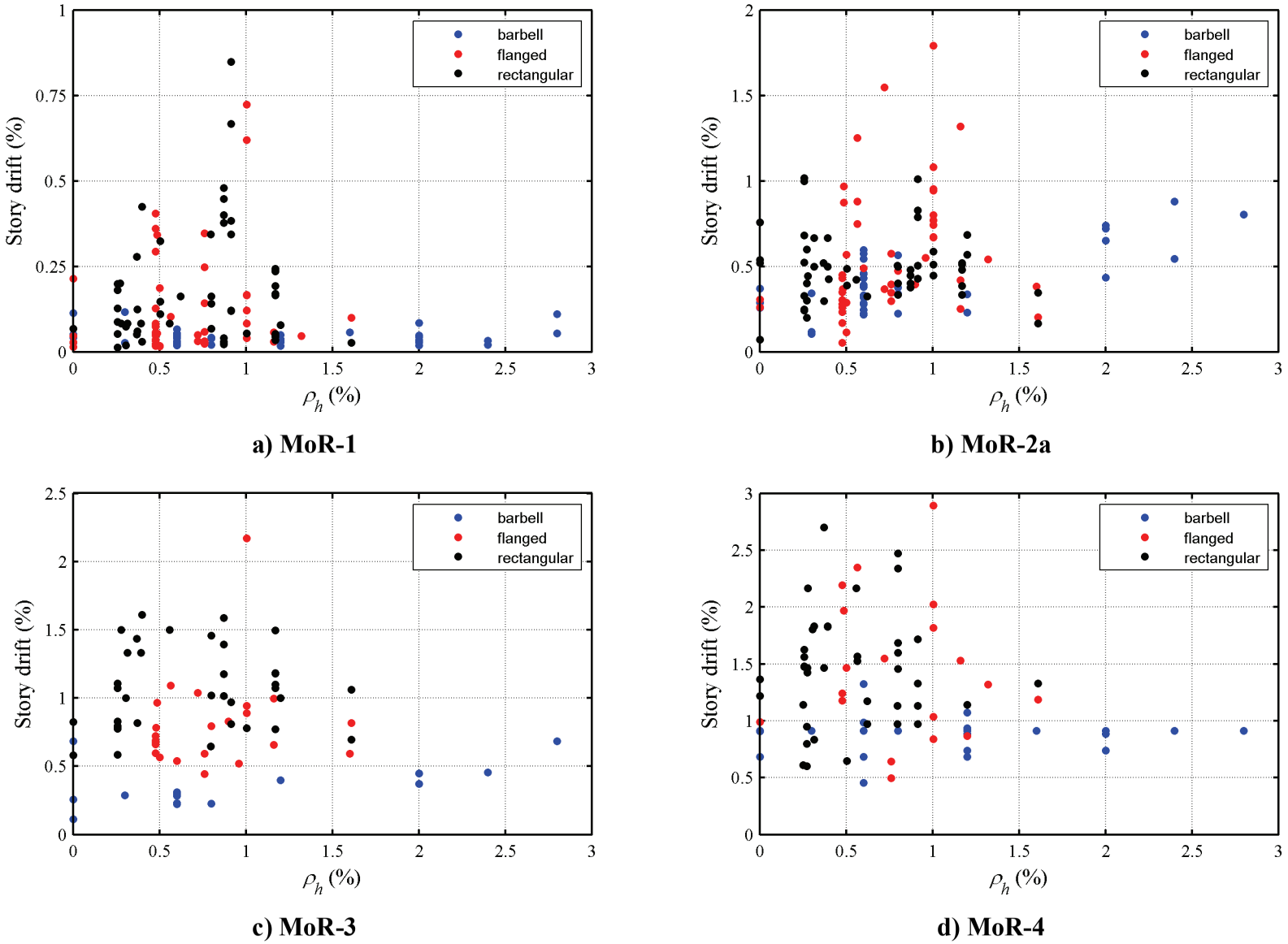

Figure 17 Variation of drift with horizontal web reinforcement ratio for different methods of repair

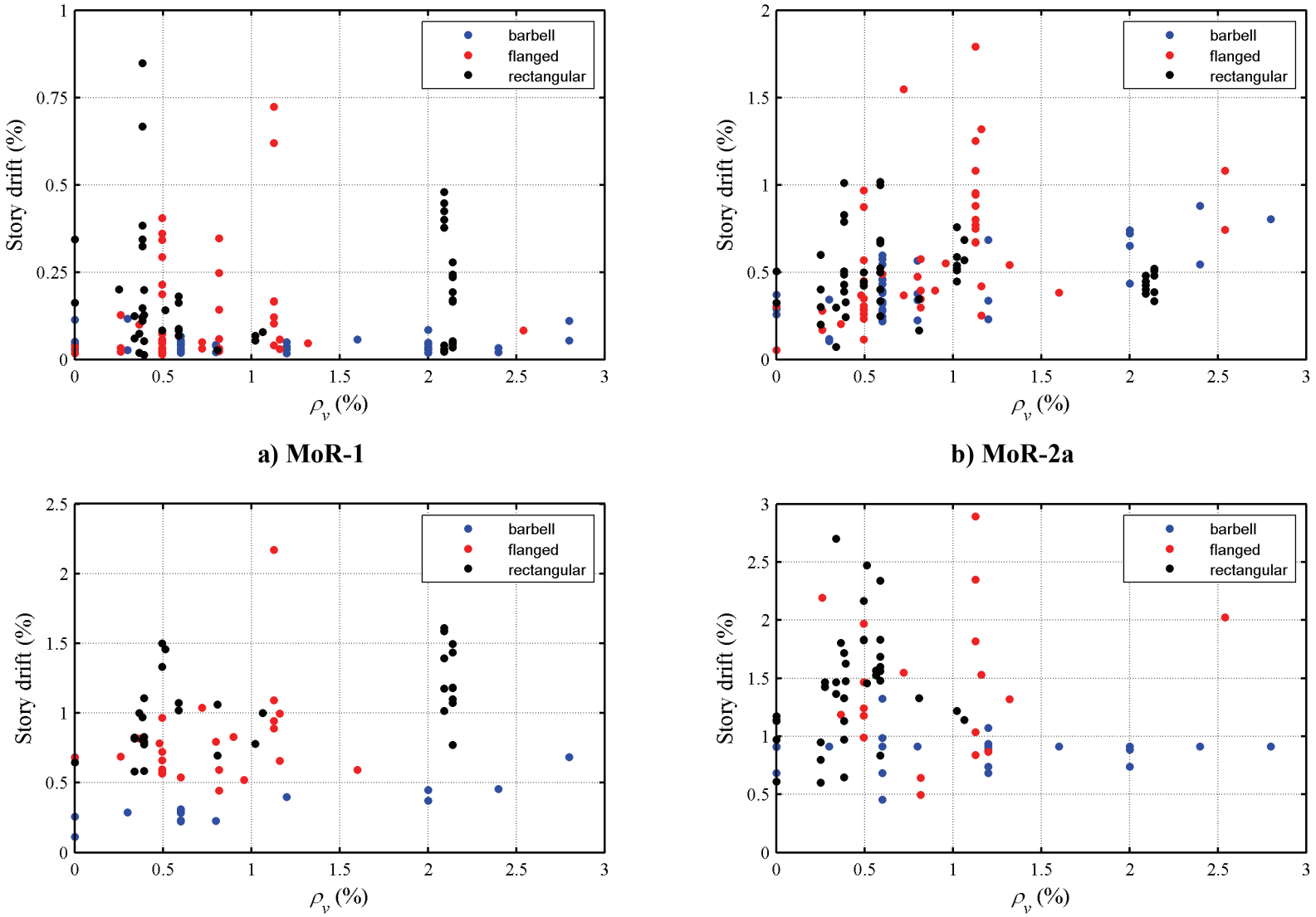

Figure 18 Variation of drift with vertical web reinforcement ratio for different methods of repair

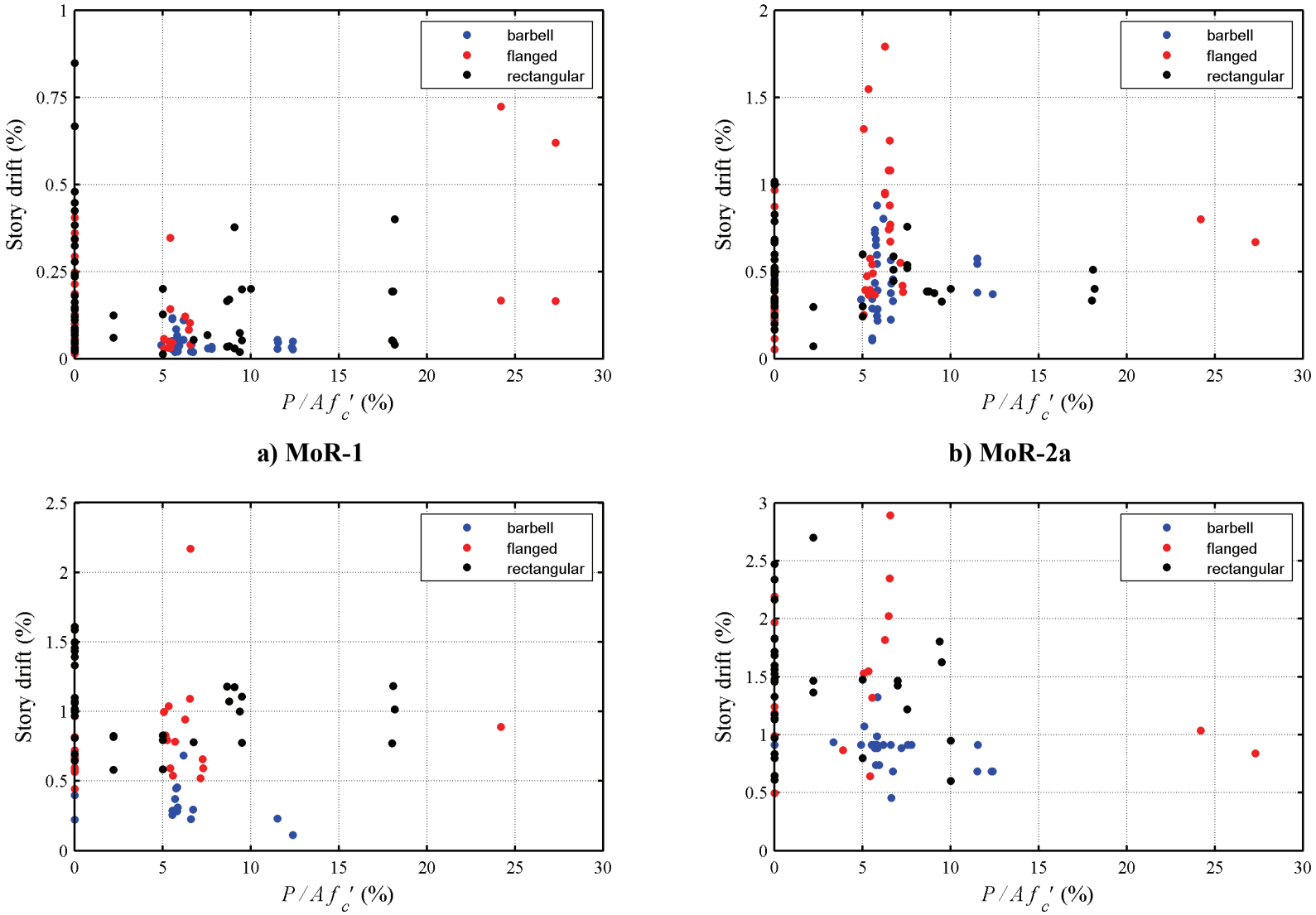

Figure 19 Variation of drift with normalized axial load for different methods of repair

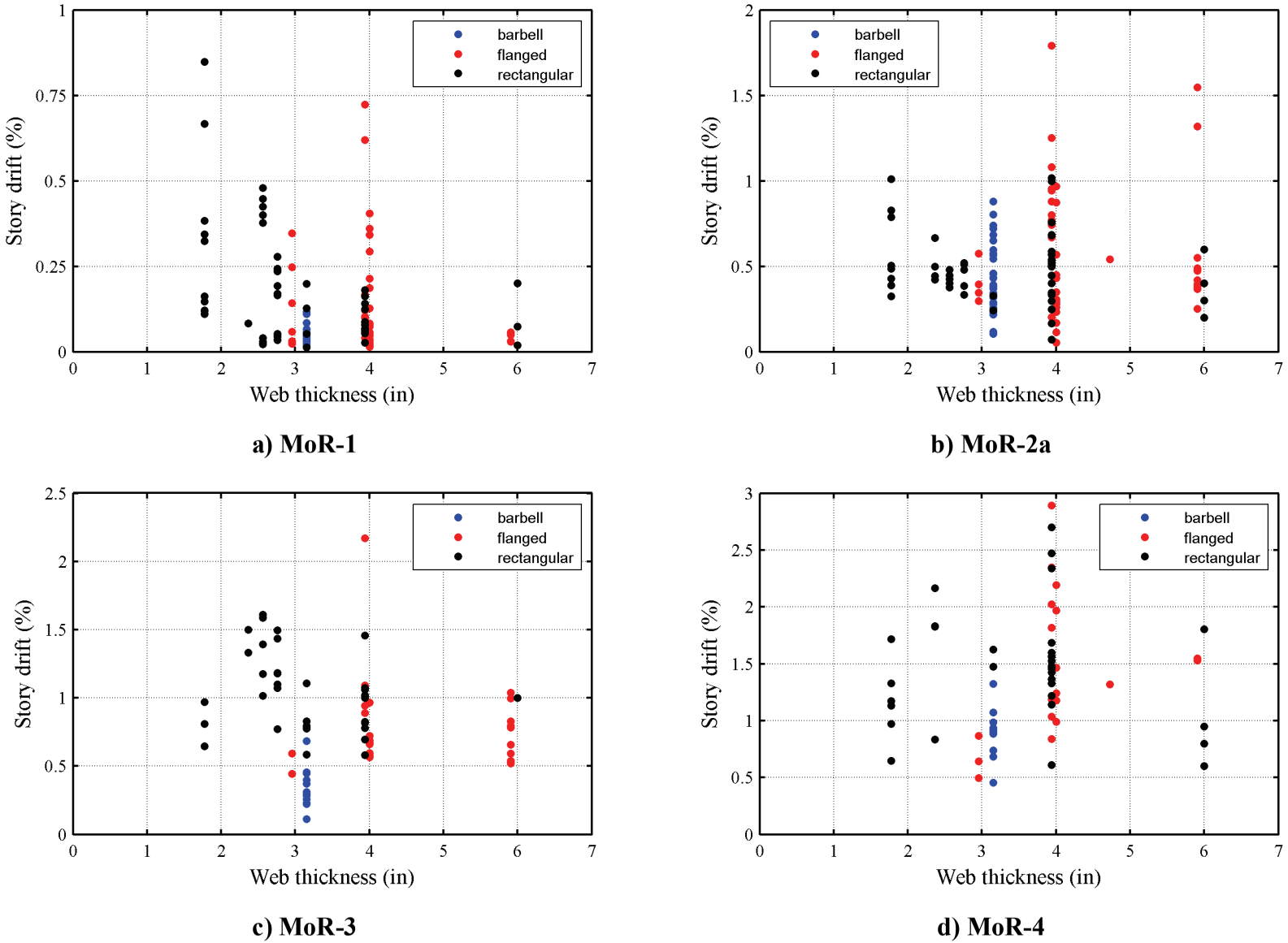

Figure 20 Variation of drift with web thickness for different methods of repair

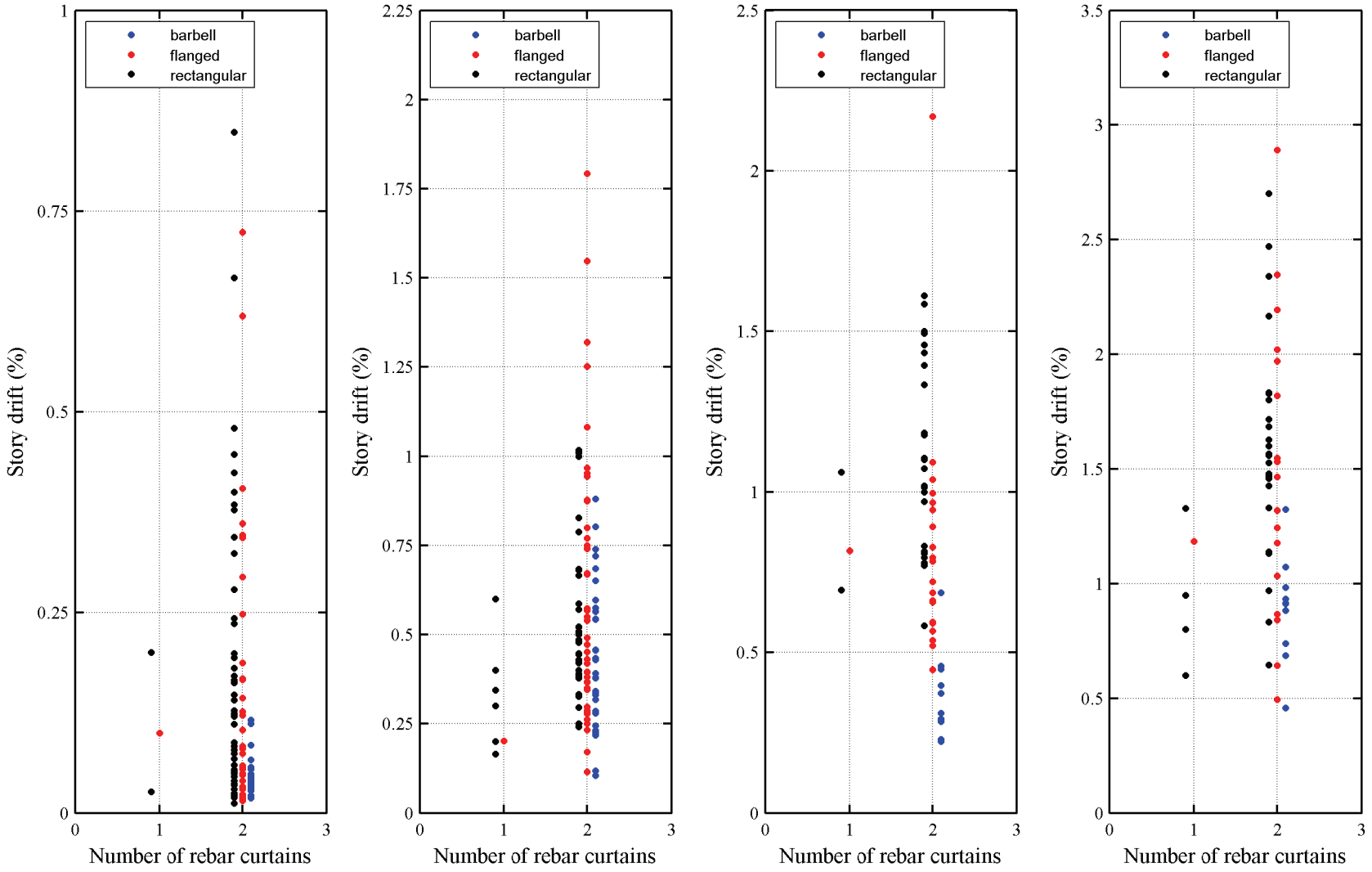

Figure 21 Variation of drift with number of rebar curtains for different methods of repair

5.7 Fragility Functions

Fragility functions that define the probability that a certain method of repair will be required conditional on story drift are developed in this section. The damage states, which are associated with specific methods of repairs (see Section 4), are used as the basis for collecting the damage data. The data characterization methods discussed in Section 5.2 are used to group the available damage data.

This section utilizes the distributions summarized in Section 5.3 to fit the damage data using the method of maximum likelihood (see Section 5.4). Fragility functions are generated for each type of wall geometry.

5.7.1 Fragility Functions Developed Using Method 1

Method 1 utilizes all available damage data for each method of repair. The distribution parameters (as defined in Section 5.3) estimated using the *method of maximum likelihood* are presented in Table 11 for rectangular, barbell and flanged walls. Results for the K-S (all distributions) and Lilliefors (lognormal distribution only) goodness-of-fit tests are presented in Table 12 and Table 13. The goodness-of-fit tests of Table 12 and Table 13 were conducted at the 5% significance level.

The data presented in Table 12 include the K-S test parameter (D), decision on the null hypothesis that the data comes from the hypothesized probability distribution (A = Accept, R = Reject), p value of the test and the critical test parameter (D_{crit}). As noted previously, if $D \le D_{crit}$, the null hypothesis (H_0) is accepted. The null hypothesis for the K-S test is rejected in one of the fourteen cases (3 wall geometries x 5 MoR except for MoR-2b and barbell walls) for the gamma, Weibull and lognormal distributions (barbell walls, MoR4),

Wall Geometry	MoR	Distribution Parameters							
		lognormal		gamma		Weibull		beta	
		θ	β	k	λ	k	λ	α	β
Rectangular	1	0.11	0.92	1.40	8.37	0.18	1.16	1.20	5.54
	2a	0.43	0.43	6.06	12.98	0.53	2.61	2.63	3.38
	2b	0.54	0.36	8.49	14.76	0.64	3.26	2.16	2.79
	3	1.03	0.28	13.43	12.59	1.18	4.09	1.39	1.58
	4	1.30	0.37	7.69	5.52	1.56	3.00	1.70	2.95
Barbell	1	0.04	0.47	4.27	101.72	0.05	1.92	0.87	2.47
	2a	0.38	0.50	4.61	10.76	0.48	2.37	2.26	3.20
	3	0.32	0.45	5.29	15.05	0.40	2.37	1.97	2.17
	4	0.87	0.17	25.20	28.82	0.94	6.24	3.95	4.20
Flanged	1	0.07	1.03	1.02	8.08	0.12	0.94	0.68	3.85
	2a	0.48	0.68	2.54	4.32	0.66	1.66	2.15	4.94
	2b	0.71	0.34	8.78	11.69	0.84	3.28	0.36	0.40
	3	0.75	0.32	8.79	11.00	0.90	2.42	0.69	2.66
	4	1.32	0.44	5.54	3.82	1.64	2.56	1.01	1.52

Table 11 Distribution parameters computed using Method 1

and rejected two times for the beta distribution (rectangular walls, MoR-2; barbell walls, MoR-4). The D statistic for the K-S test represent the maximum absolute difference between the empirical CDF and the theoretical CDF. Therefore, it is a measure of the deviation between the reported data and the hypothesized CDF. In Table 12, the yellow shaded cells represented the smallest D for the K-S test conducted on the corresponding wall geometry and method of repair. For six of the fourteen cases investigated, the lognormal distribution yields the smallest values of D. In another three instances, the value of D for the lognormal distribution is only marginally (<10%) larger than the smallest value of D. The lognormal distribution is therefore judged to be the best of the distributions considered here. Table 13 presents the Lilliefors goodness-of-fit test results on the lognormal distribution. The Lilliefors test yields smaller values of D_{crit} than for the K-S test for a given sample size and significance level (see Section 6.5.5). As seen in Table 13, the lognormal distribution fails

Wall geometry	MoR	K-S Test Results											
		D_{crit}	lognormal			gamma			Weibull			beta		
			p	H_0	D	p	H_0	D	p	H_0	D	p	H_0	D
Rectangular	1	0.166	0.911	A	0.068	0.492	A	0.102	0.498	A	0.101	0.237	A	0.126
	2a	0.161	0.327	A	0.113	0.508	A	0.097	0.193	A	0.128	0.038	R	0.167
	2b	0.294	0.288	A	0.213	0.399	A	0.194	0.720	A	0.150	0.491	A	0.180
	3	0.215	0.627	A	0.119	0.556	A	0.126	0.535	A	0.128	0.656	A	0.116
	4	0.203	0.678	A	0.108	0.892	A	0.086	0.921	A	0.082	0.815	A	0.095
Barbell	1	0.201	0.770	A	0.098	0.558	A	0.117	0.273	A	0.147	0.348	A	0.138
	2a	0.221	0.903	A	0.093	0.946	A	0.086	0.81	A	0.104	0.632	A	0.122
	3	0.338	0.885	A	0.145	0.857	A	0.151	0.725	A	0.172	0.132	A	0.290
	4	0.234	0.002	R	0.327	0.002	R	0.327	0.005	R	0.297	0.005	R	0.298
Flanged	1	0.194	0.410	A	0.127	0.078	A	0.182	0.175	A	0.158	0.111	A	0.172
	2a	0.183	0.853	A	0.082	0.661	A	0.098	0.573	A	0.106	0.124	A	0.159
	2b	0.483	0.714	A	0.249	0.737	A	0.244	0.792	A	0.232	0.971	A	0.174
	3	0.264	0.936	A	0.104	0.730	A	0.134	0.273	A	0.194	0.241	A	0.200
	4	0.301	0.999	A	0.081	1.000	A	0.078	0.976	A	0.106	0.983	A	0.103

Table 12 K-S test results for each distribution obtained using Method 1

Wall Geometry	MoR	Lilliefors Test Results			
		D_{crit}	p	H_0	D
Rectangular	**1**	0.110	0.500	A	0.067
	2a	0.107	0.028	R	0.113
	2b	0.192	0.020	R	0.210
	3	0.142	0.214	A	0.116
	4	0.134	0.247	A	0.106
Barbell	**1**	0.132	0.381	A	0.096
	2a	0.146	0.500	A	0.090
	3	0.219	0.438	A	0.153
	4	0.154	0.001	R	0.326
Flanged	**1**	0.128	0.058	A	0.126
	2a	0.121	0.500	A	0.080
	2b	0.304	0.322	A	0.230
	3	0.173	0.500	A	0.107
	4	0.197	0.500	A	0.084

Table 13 Lilliefors results for the lognormal distribution computed using Method 1

the Lilliefors goodness-of-fit test for MoR-2a and MoR-2b for the rectangular walls and for MoR-4 for the barbell walls. Note that no outlier analysis was undertaken before processing the data.

The functions developed using lognormal distribution for each wall geometry and method of repair type can be compared using the medians (θ) and logarithmic standard deviations (β) presented in the gray shaded columns of Table 11. The standard deviations for MoR-1 are generally high, which is attributed to the use of Method 1 that includes all available damage data. The standard deviations for other methods of repair are generally reasonable. ATC-58 [ATC (2008)] qualifies the fragility functions that pass the Lilliefors goodness-of-fit test and yield logarithmic standard deviations (β) of less than 0.6 as *high quality*. One interesting observation is that for barbell walls, MoR-3 precedes MoR-2a, that is, the median drift associated for MoR-3 is less than that of MoR-2a. This anomaly is attributed to the

characteristics of the barbell wall data used herein, namely, very low-aspect ratio and heavy web reinforcement in most cases. Figure 22, Figure 23, and Figure 24 present the empirical and theoretical fragility functions for rectangular, barbell and flanged walls, respectively.

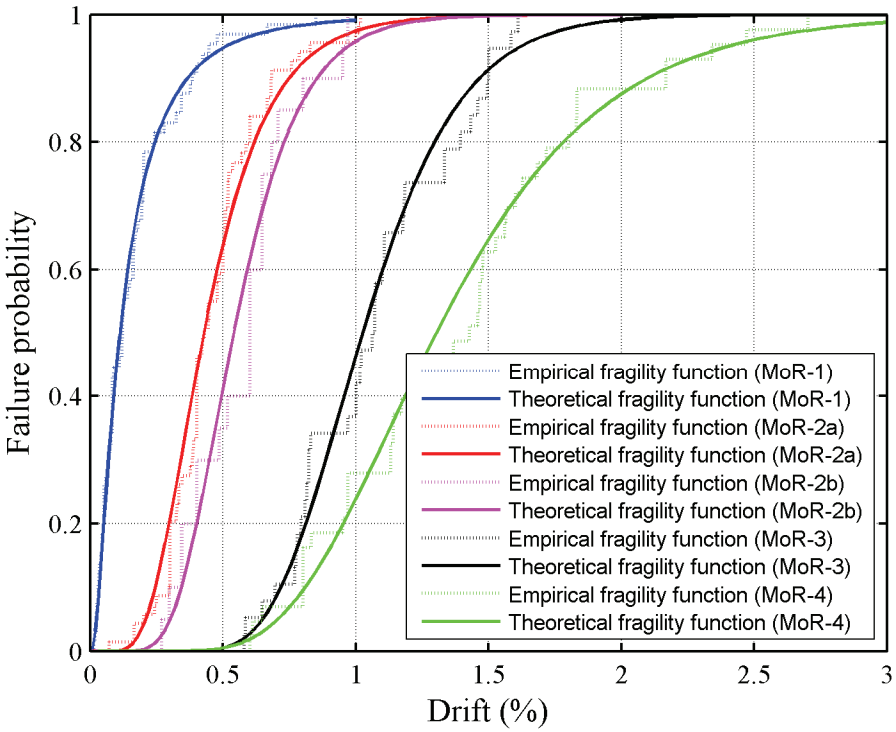

Figure 22 Method 1 fragility functions for rectangular walls

5.7.2 Fragility Functions Developed Using Method 2

Method 2 utilizes the damage data with the smallest demand parameter (drift) for each method of repair of each specimen. The distribution parameters are presented in Table 14 for rectangular, barbell and flanged walls. Results for the K-S (all distributions) and Lilliefors (lognormal distribution only) goodness-of-fit tests are presented in Table 15 and Table 16 at the 5% significance level. As seen in Table 15, the null hypothesis for the K-S test is rejected once (rectangular walls, MoR-4) for each distribution type for Method 2.

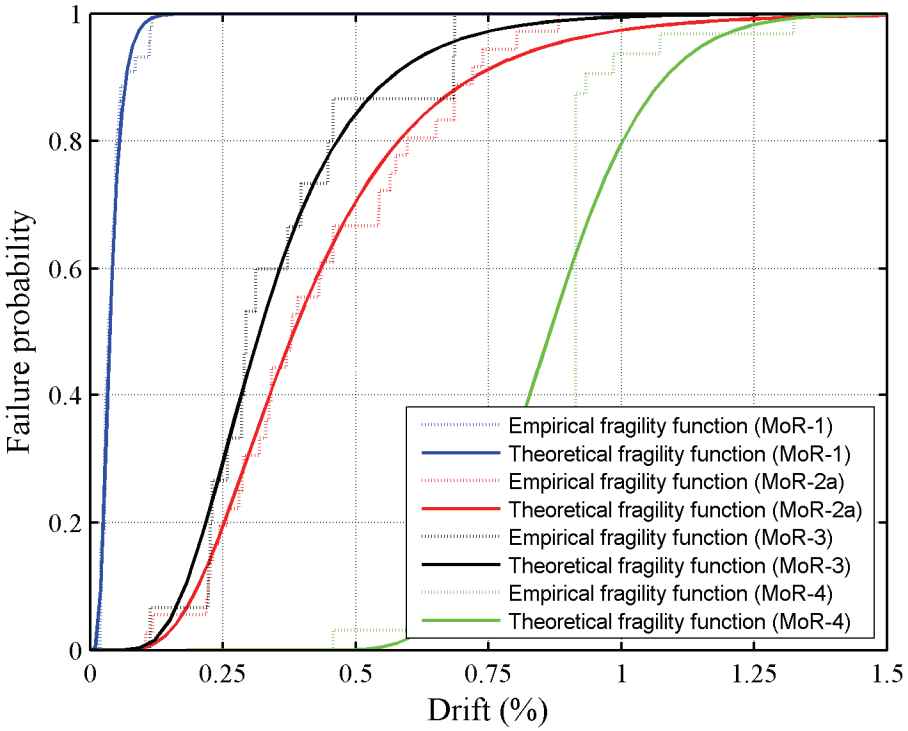

Figure 23 Method 1 fragility functions for barbell walls

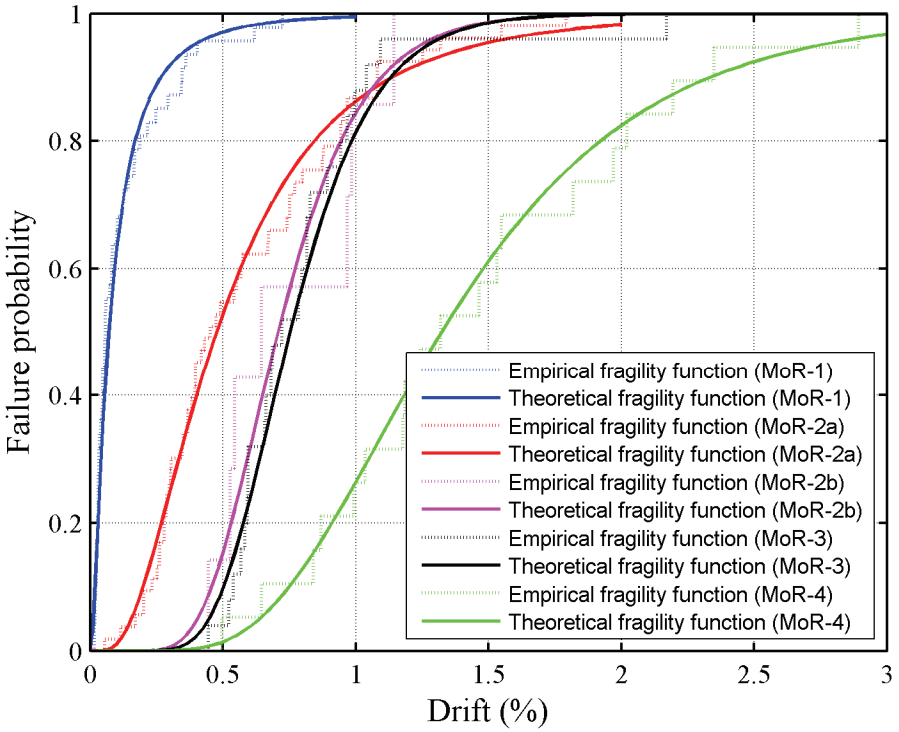

Figure 24 Method 1 fragility functions for flanged walls

Wall Geometry	MoR	Distribution Parameters							
		lognormal		gamma		Weibull		beta	
		θ	β	k	λ	k	λ	α	β
Rectangular	1	0.07	0.81	1.58	15.04	0.11	1.18	2.13	15.34
	2a	0.40	0.42	6.81	15.88	0.48	3.01	5.78	6.34
	2b	0.54	0.36	8.49	14.76	0.64	3.26	2.16	2.79
	3	1.05	0.30	11.79	10.75	1.21	4.03	1.27	1.32
	4	1.25	0.35	9.10	6.90	1.47	3.55	2.15	2.96
Barbell	1	0.03	0.31	10.11	316.82	0.04	3.19	1.32	2.48
	2	0.33	0.49	4.48	11.93	0.43	2.21	0.90	1.42
	3	0.32	0.45	5.29	15.05	0.40	2.37	1.97	2.17
	4	0.87	0.17	35.22	40.12	0.94	6.24	3.95	4.20
Flanged	1	0.04	0.79	1.71	29.17	0.06	1.29	0.65	1.48
	2a	0.36	0.62	3.27	7.71	0.48	2.03	3.81	5.45
	2b	0.72	0.37	7.79	10.14	0.86	3.22	0.33	0.35
	3	0.75	0.32	8.45	10.58	0.90	2.39	0.65	2.51
	4	1.32	0.44	5.54	3.82	1.64	2.56	1.01	1.52

Table 14 Distribution parameters computed using Method 2

In Table 15, the yellow shaded cells identify the smallest values of D for the K-S test for each wall geometry and method of repair. For five of the fourteen cases investigated, the lognormal distribution yields the smallest D. Accordingly, the lognormal distribution is used to develop fragility curves for squat reinforced concrete walls. Table 16 presents the Lilliefors goodness-of-fit test results. The lognormal distribution fails the goodness-of-fit test for MoR-2a, MoR-2b and MoR-4 for rectangular walls and MoR-4 for barbell walls.

The logarithmic standard deviations corresponding to MoR-1 are generally high but less than those observed for Method 1. The logarithmic standard deviations for MoR-2a, MoR-2b, MoR-3 and MoR-4 are less than 0.60 except for the flanged walls and MoR-2a (β = 0.62). Similar to that observed for Method 1, MoR-3 precedes MoR-2a for barbell walls and MOR-2a. Figure 25, Figure 26, and Figure 27 present the empirical and theoretical fragility functions developed using data characterization Method 2.

Wall geometry	MoR	K-S Test Results											
		D_{crit}	lognormal			gamma			Weibull			beta		
			p	H_0	D	p	H_0	D	p	H_0	D	p	H_0	D
Rectangular	1	0.205	0.902	A	0.086	0.304	A	0.147	0.365	A	0.139	0.234	A	0.156
	2a	0.203	0.266	A	0.150	0.526	A	0.121	0.369	A	0.137	0.555	A	0.119
	2b	0.294	0.288	A	0.213	0.399	A	0.194	0.720	A	0.150	0.491	A	0.180
	3	0.242	0.752	A	0.120	0.766	A	0.119	0.781	A	0.117	0.852	A	0.108
	4	0.215	0.318	A	0.152	0.440	A	0.138	0.717	A	0.111	0.088	A	0.198
Barbell	1	0.246	0.662	A	0.132	0.529	A	0.146	0.398	A	0.162	0.607	A	0.138
	2a	0.309	0.869	A	0.136	0.893	A	0.131	0.785	A	0.149	0.386	A	0.206
	3	0.338	0.885	A	0.145	0.857	A	0.151	0.725	A	0.172	0.132	A	0.290
	4	0.234	0.002	R	0.327	0.002	R	0.317	0.005	R	0.297	0.005	R	0.298
Flanged	1	0.301	0.568	A	0.174	0.357	A	0.206	0.419	A	0.196	0.290	A	0.218
	2a	0.254	0.881	A	0.110	0.993	A	0.081	0.945	A	0.099	0.299	A	0.182
	2b	0.519	0.609	A	0.291	0.637	A	0.285	0.584	A	0.297	0.980	A	0.180
	3	0.269	0.910	A	0.111	0.835	A	0.123	0.282	A	0.196	0.226	A	0.207
	4	0.301	0.999	A	0.081	1.000	A	0.078	0.976	A	0.106	0.983	A	0.103

Table 15 K-S test results for each distribution computed using Method 2

Wall Geometry	MoR	Lilliefors Test Results			
		D_{crit}	p	H_0	D
Rectangular	1	0.135	0.500	A	0.087
	2a	0.134	0.015	R	0.151
	2b	0.192	0.020	R	0.210
	3	0.159	0.364	A	0.116
	4	0.142	0.029	R	0.150
Barbell	1	0.161	0.194	A	0.134
	2a	0.201	0.417	A	0.143
	3	0.219	0.438	A	0.153
	4	0.154	0.001	R	0.326
Flanged	1	0.197	0.148	A	0.171
	2a	0.167	0.500	A	0.110
	2b	0.324	0.194	A	0.270
	3	0.176	0.500	A	0.109
	4	0.197	0.500	A	0.084

Table 16 Lilliefors results for the lognormal distribution computed using Method 2

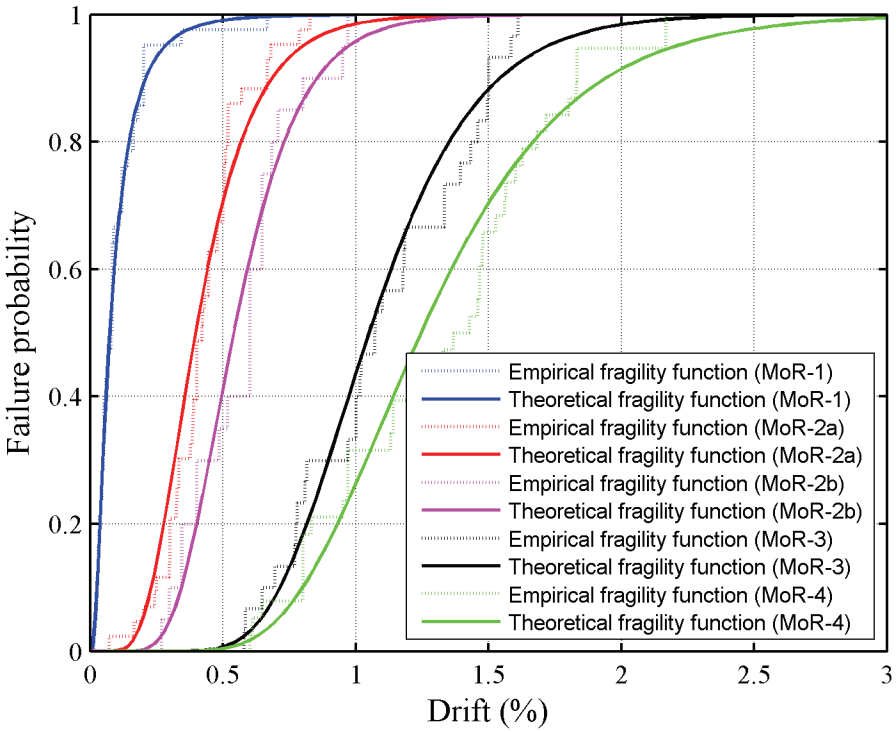

Figure 25 Method 2 fragility functions for rectangular walls

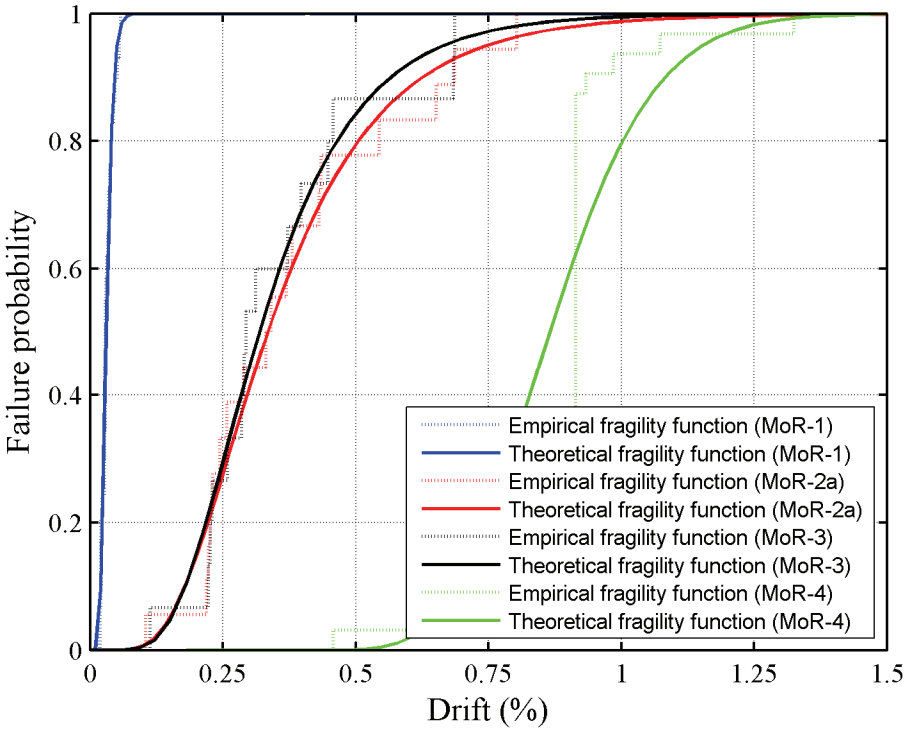

Figure 26 Method 2 fragility functions for barbell walls

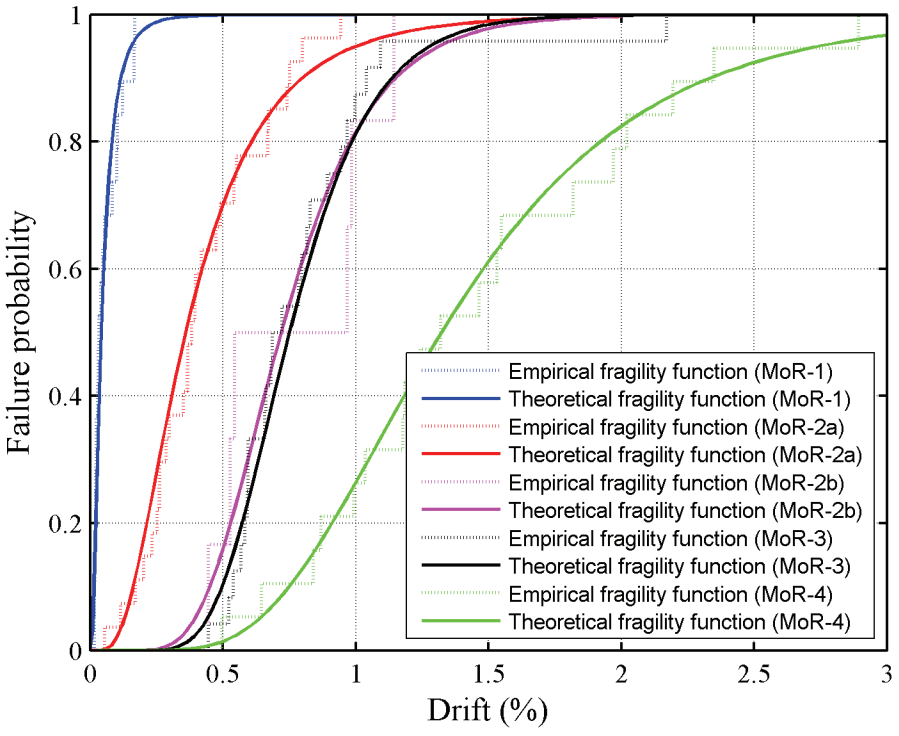

Figure 27 Method 2 fragility functions for flanged walls

6 Fragility Function Recommendations

6.1 Probability Distribution

The fragility data presented in Section 5.7 reveal that the lognormal distribution is the best of the four distributions considered for representing fragility functions for squat reinforced concrete walls for both Method 1 and Method 2.

6.2 Data Characterization

The fragility curves obtained using the lognormal distribution differ only modestly for Method 1 and Method 2 (see the gray shaded cells in Table 11 and Table 14). The dispersions for Method 1 are generally greater than those for Method 2 for the four methods of repair. Accordingly, fragility functions developed using Method 2 are used.

Table 17, based principally on Table 14, lists the values of median and dispersion obtained using the lognormal distribution and Method 2 for the three wall geometries and four methods of repair. Two significant figures are used to report median (θ) drift. Two decimal digits are used for dispersion (β).

6.3 Evaluation of Damage States

6.3.1 Damages States Associated with Reinforcement Yielding for MoR-2a

MoR-2a uses reinforcement yielding data (DS2.1, DS2.2 and DS2.3) together with DS2.4a and DS2.5a that are associated with crack widths of 0.5+ mm. This assumption is evaluated herein by fitting lognormal distribution using Method 2 to a) reinforcement yielding data (DS2.1, DS2.2 and DS2.3), and crack width data (DS2.4a and DS2.5a). Table 18 presents the parameters of the distribution. The parameters for barbell walls and DS2.4a and DS2.5a cannot be obtained due to a lack of data. For rectangular and flanged walls, the medians

Wall geometry	MoR	θ	β
Rectangular	1	0.07	0.81
	2a	0.40	0.42
	2b	0.54	0.36
	3	1.05	0.30
	4	1.25	0.35
Barbell[1]	1	0.03	0.31
	2a	0.33	0.49
	3	0.32	0.45
	4	0.87	0.17
Flanged	1	0.04	0.79
	2a	0.36	0.62
	2b	0.72	0.37
	3	0.75	0.32
	4	1.32	0.44

1. Data not presented for MoR-2b; see footnote in Table 10.

Table 17 Lognormal distribution parameters calculated using Method 2

calculated using yielding data (DS2.1, DS2.2 and DS2.3) and crack width data (DS2.4a and DS2.5a) are in close agreement.

The data of Table 18 support the use of reinforcement yielding data and crack width data for MoR-2a.

6.3.2 Damage States Associated with Supplemental Criteria for MoR-4

Two supplemental criteria are suggested for MoR-4 to aid in identification of damage for cases where the reported data is insufficient to make an assessment. The first supplemental criterion, SC_1, serves to identify drift at sliding shear failure. The second criterion, SC_2, is intended to the identify threshold drift for wall replacement for walls that fail under diagonal tension or compression, for cases where the drift at failure is unclear. The drifts identified using the supplemental criteria are presented in Appendix A.

Wall geometry	Damage states	θ	β
Rectangular	DS2.1, DS2.2, DS2.3	0.41	0.31
	DS2.4a, DS2.5a	0.42	0.54
	DS2.1, DS2.2, DS2.3, DS2.4a, DS2.5a	0.40	0.42
Barbell	DS2.1, DS2.2, DS2.3	0.31	0.49
	DS2.4a, DS2.5a	N/A[1]	N/A
	DS2.1, DS2.2, DS2.3, DS2.4a, DS2.5a	0.33	0.49
Flanged	DS2.1, DS2.2, DS2.3	0.41	0.51
	DS2.4a, DS2.5a	0.40	0.84
	DS2.1, DS2.2, DS2.3, DS2.4a, DS2.5a	0.36	0.62

1. Fitting is not possible since there are only 3 data points associated with these damage states.

Table 18 Lognormal distribution parameters calculated using Method 2 for MoR-2a damage states

Table 19 presents the distribution parameters for MoR-4 calculated with and without SC_1 and SC_2. As seen in the table, the use of the supplemental criteria does not significantly alter the distribution parameters. Criterion SC_1 identifies 13 data points for rectangular walls, 5 data points for flanged walls and 0 data points for barbell walls. Criterion SC_2 identifies 6 data points for flanged walls, 2 data points for barbell walls and 0 data points for rectangular walls.

The data of Table 19 shows that the use of the two supplemental criteria does not substantially modify the values of the distribution parameters. Accordingly, the recommended medians and dispersions presented below make use of supplemental criteria.

Wall geometry	SC_1	SC_2	θ	β
Rectangular	Considered	Considered	1.25	0.35
	Considered	Not considered	1.25	0.35
	Not considered	Not considered	1.15	0.40
Barbell	Considered	Considered	0.87	0.17
	Considered	Not considered	0.86	0.18
	Not considered	Not considered	0.86	0.18
Flanged	Considered	Considered	1.32	0.44
	Considered	Not considered	1.31	0.51
	Not considered	Not considered	1.27	0.61

Table 19 Effect of SC_1 and SC_2 on the MoR-4 lognormal distribution parameters for Method 2

6.4 ACI 318-08 Compliance

Eleven of the 111 test specimens (6 rectangular, 2 flanged and 3 barbell) used to develop fragility functions did not comply with the minimum reinforcement requirements ($\rho_h = \rho_v = 0.25\%$) of ACI 318-08 [ACI (2008)] for *Special Structural Walls and Concrete Beams* (Chapter 21.9). This section presents fragility functions for walls that comply with the minimum reinforcement reqirements of ACI 318-08 [ACI (2008)]. The lognormal distribution and Method 2 are used to develop the fragility functions. Results are presented in Table 20.

A comparison of the distribution parameters presented in Table 17 and Table 20 reveal that limiting the minimum web reinforcement ratios per ACI 318-08 [ACI (2008)] does not significantly affect the distribution parameters. The most significant effect is observed for MoR-2a for flanged walls for which the median drift increased from 0.36% to 0.39% and logarithmic standard deviation decreased from 0.62 to 0.51.

Wall geometry	MoR	Lognormal		Lilliefors Test Results			
		θ	β	D_{crit}	p	H_0	D
Rectangular	1	0.07	0.79	0.140	0.500	A	0.082
	2a	0.41	0.34	0.140	0.182	A	0.118
	2b	0.55	0.34	0.207	0.143	A	0.181
	3	1.09	0.27	0.164	0.338	A	0.122
	4	1.30	0.35	0.154	0.002	R	0.202
Barbell	1	0.03	0.31	0.170	0.379	A	0.123
	2a	0.34	0.53	0.219	0.500	A	0.140
	3	0.33	0.33	0.242	0.500	A	0.159
	4	0.87	0.18	0.161	0.001	R	0.327
Flanged	1	0.05	0.76	0.207	0.190	A	0.173
	2a	0.39	0.51	0.173	0.500	A	0.089
	2b	0.72	0.37	0.324	0.194	A	0.270
	3	0.76	0.33	0.184	0.500	A	0.100
	4	1.34	0.45	0.201	0.500	A	0.110

Table 20 Lognormal distribution parameters and the corresponding Lilliefors test results for squat walls that comply with the minimum reinforcement requirements of ACI 318-08 [ACI (2008)]

Given that most squat walls will likely comply with the ACI 318-08 [ACI (2008)] requirements for minimum rebar ratio, the recommended medians and dispersions presented in Section 6.5 are based on the data of Table 20.

6.5 Recommendations

6.5.1 Rectangular Walls

Table 21 presents the recommended medians and dispersions for rectangular walls. On the basis of input from the ATC-58 Project Team, MoR-2 is represented by MoR-2b, namely, cracks widths in excess of 1.0 mm. The dispersions in the fourth column of this and the following two tables are not increased for model uncertainty because a large number of

specimens were tested in a number of laboratories by different researchers and values of the variables that effect the response of low-aspect ratio walls varied widely.

MoR	Damage State	θ	β
1	DS1	0.07	0.79
2	DS2	0.55	0.34
3	DS3	1.09	0.27
4	DS4	1.30	0.35

Table 21 Distribution parameters for rectangular walls

An analysis was performed for MoR-2 wherein damage was described solely in terms of a measured maximum flexural or shear crack width of 0.06 inch and larger. For this definition of damage, the median drift angle increased from 0.55% to 0.60%.

6.5.2 Barbell Walls

Table 22 presents the recommended medians and dispersions for barbell walls. Since the median drifts for MoR-2a and MoR-3 are virtually identical, MoR-2 is set aside for barbell walls.

MoR	Damage State	θ	β
1	DS1	0.03	0.31
3	DS3	0.33	0.33
4	DS4	0.87	0.18

Table 22 Distribution parameters for barbell walls

6.5.3 Flanged Walls

Table 23 presents the recommended medians and dispersions for flanged walls. For the reason given in Section 6.5.1, MoR-2 is represented by MoR-2b. However, given that the

median drifts for MoR-2 (=0.72%) is virtually identical to that for MoR-3 (=0.76%), MoR-2 is set aside for flanged walls.

MoR	Damage State	θ	β
1	DS1	0.05	0.76
3	DS3	0.76	0.33
4	DS4	1.34	0.45

Table 23 Distribution parameters for flanged walls

7 Scopes of Repair

To establish consequence functions and costs of repair, a list of repair activities must be assigned to each method of repair. Such lists are presented below for methods of repair MoR-1 through MoR-4.

7.1 MoR-1, Cosmetic Repair

Cosmetic repairs are made when the residual crack widths are relatively narrow and no structural repair is deemed necessary. The main scope of this method of repair is limited to the repair of surface finishes to restore the aesthetic appearance, maintain fire resistance and prevent water infiltration into the wall, [ATC (1998a)]. A list of repair activities isn't provided for MoR-1 because the repair is not structural.

7.2 MoR-2, Epoxy Injection

Epoxy injection is widely used to restore the stiffness and strength of cracked concrete components. Structural repair using epoxy injection involves the following steps, which assume that the to-be-repaired wall is in a commercial office building.

1. Relocate all office equipment and furniture within 6 ft. of the wall, on both sides of the wall. Install protective covers on the floor finishes.
2. Remove architectural finishes over the height and length of the wall, on both sides of the wall.
3. Relocate mechanical, electrical and plumbing (MEP) systems within 6 ft. of the damaged wall.
4. Prepare and injection grout 300 ft. of crack per 100 ft^2 of wall panel for rectangular cross sections. (See Appendix B for additional information on calculation of the suggested cracks lengths.)
5. Reinstall/return all office equipment, architectural finishes, furniture, and MEP systems.

7.3 MoR-3, Partial Wall Replacement

Partial wall replacement (MoR-3) includes a) removal and replacement of damaged concrete and rebar, and b) epoxy injection of cracks to restore component strength and stiffness. Such repair involves the following steps that assume a) the wall is in a commercial office building, and b) wall replacement does not involve shoring of columns and floor slabs. The scope of repair is not additional to that of MoR-2.

1. Relocate all office equipment and furniture within 6 ft. of the wall, on both sides of the wall. Install protective covers on the floor finishes and adjacent curtain wall system (where occurs).
2. Remove architectural finishes over the height and length of the wall, on both sides of the wall.

3. Relocate MEP systems within 6 ft. of the damaged wall.

4. Prepare and injection grout 330 ft. of crack per 100 ft^2 of wall panel for walls with rectangular cross sections and 310 ft. of crack per 100 ft^2 of wall panel for walls with flanged or barbell cross sections. (See Appendix B for additional information on calculation of the suggested cracks lengths.)

5. Remove 15 ft^2 per 100 ft^2 of wall panel and 10 1-ft. long sections of #8 buckled rebar. (See Appendix B for additional information on the calculation of the area of wall panel to be removed.)

6. Replace buckled rebar with new rebar, attached to exposed ends of existing rebar with mechanical splices; provide 8 #4 seismic ties at 4 in. on center at each end of the wall; re-bend 16 horizontal rebar in the web of the wall around new rebar.

7. Install formwork and cast new 5000 psi concrete into the pockets cut in step 5.

8. Strip formwork, remove all construction equipment, and reinstall/return all office equipment, architectural finishes, furniture, and MEP systems.

7.4 MoR-4, Wall Replacement

Method of repair MoR-4 includes replacement of the damaged wall panel and is similar to Structural Repair 5 (SR5) of FEMA 308 [ATC (1998a)]. MoR-4 involves the following steps, which assume that a) the wall is in a commercial office building, and b) wall removal and replacement in 5-ft. increments such that shoring of columns and floor slabs above is not required.

1. Relocate all office equipment and furniture within 10 ft. of the wall, on both sides of the wall. Install protective covers on the floor finishes and adjacent curtain wall system (where occurs). Relocate MEP systems within 10 ft. of the damaged wall.
2. Remove architectural finishes over the height and length of the wall, on both sides of the wall.
3. Remove and replace the damaged reinforced concrete in 5-ft. segments along the length along the wall.
4. Install new reinforcement as follows:
    a. 12#9 A706 rebar in the boundary zone at each end of the wall; attach new rebar to existing using mechanical splices
    b. #4 A706 double sets of seismic ties at 4 in. on center in each boundary zone;
    c. #4 A706 rebar at 6 in. on center, each face, each way; lap splice new vertical bars to existing at the head of the wall; drill and epoxy grout #4 bars into wall/foundation below at 6 in. on center to match new rebar above. Horizontal rebar to be anchored in new boundary zones with seismic hooks or lapped 24 in. with horizontal bars in adjacent wall panels.
5. Form new wall panel and cast 5000 psi concrete in 3-ft. lifts; leave a 1-in. gap at the underside of the wall above for grouting 24 hours after the wall panel is cast. Strip formwork 48 hours after casting. Commence work on a new panel after concrete has achieved compressive strength of 3000 psi.
6. Remove all construction equipment and reinstall/return all office equipment, architectural finishes, furniture, and MEP systems.

8 References

ACI Committee 546, 2004, "Concrete Repair Guide (ACI 546R-04)," American Concrete Institute, Farmington Hills, MI, 53 pp.

ACI Committee 318, 2008, "Building Code Requirements for Structural Concrete and Commentary (ACI 318-08)," American Concrete Institute, Farmington Hills, MI, 467 pp.

AIJ, 1985a, "Load-Deflection Characteristics of Nuclear Reactor Building Structures: Parts 37-38-39-40," *Summaries of Technical Papers of Annual Meeting, B, Structures I*, Architectural Institute of Japan, Japan. (in Japanese)

AIJ, 1985b, "Load-Deflection Characteristics of Nuclear Reactor Building Structures: Parts 8-9-10," *Summaries of Technical Papers, Structural Division*, Vol. 58, Architectural Institute of Japan, Japan. (in Japanese)

AIJ, 1986a, "Load-Deflection Characteristics of Nuclear Reactor Building Structures: Parts 59-60-61," *Summaries of Technical Papers of Annual Meeting, B, Structures I*, Architectural Institute of Japan, Japan. (in Japanese)

AIJ, 1986b, "Load-Deflection Characteristics of Nuclear Reactor Building Structures: Parts 62-63," *Summaries of Technical Papers of Annual Meeting, B, Structures I*, Architectural Institute of Japan, Japan. (in Japanese)

AIJ, 1986c, "Load-Deflection Characteristics of Nuclear Reactor Building Structures: Parts 21-22," *Summaries of Technical Papers, Structural Division*, Vol. 59, Architectural Institute of Japan, Japan. (in Japanese)

ATC, 1998a, "Repair of Earthquake Damaged Concrete and Masonry Wall Buildings (FEMA 308)," Federal Emergency Management Agency, Washington, DC, 66 pp.

ATC, 1998b, "Evaluation of Earthquake Damaged Concrete and Masonry Buildings - Basic Procedures Manual (FEMA 306)," Federal Emergency Management Agency, Washington, DC, 250 pp.

ATC, 2008, "Guidelines for Seismic Performance Assessment of Buildings (ATC-58)," Applied Technology Council, <http://www.atcouncil.org/atc-58.shtml>.

Barda, F., 1972, "Shear Strength of Low-Rise Walls with Boundary Elements," PhD Dissertation, Lehigh University, Bethlehem, PA.

Benjamin, J. R., and Cornell, C. A., 1970, *Probability, Statistics, and Decision for Civil Engineers*, McGraw-Hill, New York, 684 pp.

Brown, P. C., and Lowes, L. N., 2007, "Fragility Functions for Modern Reinforced-Concrete Beam-Column Joints," *Earthquake Spectra*, Vol. 23, No. 2, May, pp. 263-289.

Brown, P. C., 2008, "Probabilistic Earthquake Damage Prediction for Reinforced Concrete Building Components," MS Thesis, Department of Civil and Environmental Engineering, University of Washington, Seattle, WA, 173 pp.

Greifenhagen, C.; Papas, D.; and Lestuzzi, P., 2005, "Static-Cyclic Tests on Reinforced Concrete Shear Walls with Low Reinforcement Ratios," *Report* No. N4, School of Architecture, Civil and Environmental Engineering, Ecole Polytechnique Federale De Lausanne, Lausanne, Switzerland, 113 pp.

Gulec, C. K., 2009, "Performance-Based Assessment and Design of Squat Reinforced Concrete Shear Walls," PhD Dissertation, Department of Civil, Structural and Environmental Engineering, University at Buffalo, Buffalo, NY.

Hidalgo, P. A.; Ledezma, C. A.; and Jordan, R. M., 2002, "Seismic Behavior of Squat Reinforced Concrete Shear Walls," *Earthquake Spectra*, EERI, Vol. 18, No. 2, pp. 287-308.

Kitada, Y.; Akino, K.; Terada, K.; Aoyama, H.; and Miller, A., 1997, "Report on Seismic Shear Wall International Standard Problem Organized by OECD/NEA/CSNI," *Proceedings*, Fourteenth International Conference on Structural Mechanics in Reactor Technology, HKW/1, Lyon, France.

Lefas, I. D.; Kotsovos, M. D.; and Ambraseys, N. N., 1990, "Behavior of Reinforced Concrete Structural Walls: Strength, Deformation Characteristics, and Failure Mechanism," *ACI Structural Journal*, Vol. 87, No. 1, Jan.-Feb., pp. 23-31.

Lilliefors, H. W., 1967, "On the K-S Test for Normality with Mean and Variance Unknown," *Journal of American Statistical Association*, Vol. 62, June, pp. 399-402.

Lopes, M. S., and Elnashai, A. S., 1991, "Seismic Behaviour of RC Walls with Low Shear Ratio," *Report* No. 91-9, ESEE Research Report, Civil Engineering Department, Imperial College, London, UK, 439 pp.

Lowes, L. N., and Li, J., 2008, "Fragility Curves for Reinforced Concrete Special and Intermediate Moment Frames," Report to ATC-58.

Maier, J., and Thürlimann, B., 1985, "Bruchversuche an Stahlbetonscheiben," Institut für Baustatik und Konstruktion, Eidgenössische Technische Hochschule (ETH) Zürich, Zürich, Switzerland, 130 pp. (in German)

Massone, L. M., 2006, "RC Wall Shear-Flexure Interaction: Analytical and Experimental Responses," PhD Dissertation, Department of Civil and Environmental Engineering, University of California, Los Angeles, CA, 398 pp.

Mohammadi-Doostdar, H., 1994, "Behavior and Design of Earthquake Resistant Low-Rise Shear Walls," Department of Civil Engineering, University of Ottawa
Ottawa, ON, Canada, 234 pp.

Pagni, C. A., and Lowes, L. N., 2006, "Fragility Functions for Older Reinforced Concrete Beam Column Joints," *Earthquake Spectra*, EERI, Vol. 22, No. 1, pp. 215-238.

Palermo, D., and Vecchio, F. J., 2002, "Behavior and Analysis of Reinforced Concrete Walls Subjected to Reversed Cyclic Loading," *Report* No. 2002-01, Department of Civil Engineering, University of Toronto, Toronto, ON, Canada, 351 pp.

Park, Y. J., and Ang, A. H. S., 1985, "Mechanistic Seismic Damage Model for Reinforced-Concrete," *Journal of Structural Engineering*, ASCE, Vol. 111, No. 4, pp. 722-739.

Pilakoutas, K., 1991, "Earthquake Resistant Design of Reinforced Concrete Walls," *Report* No. 91-4, ESEE Research Report, Civil Engineering Department, Imperial College, London, UK, 360 pp.

Pilette, F. C., 1987, "Behavior of Earthquake Resistant Squat Shear Walls," MS Thesis, Department of Civil Engineering, University of Ottawa, Ottawa, ON, Canada, 177 pp.

Saito, H.; Kikuchi, R.; Kanechika, M.; and Okamoto, K., 1989, "Experimental Study on the Effect of Concrete Strength on Shear Wall Behavior," *Proceedings*, Tenth International Conference on Structural Mechanics in Reactor Technology, H08/05, Anaheim, CA.

Salonikios, T. N.; Kappos, A. J.; Tegos, I. A.; and Penelis, G. G., 1999, "Cyclic Load Behavior of Low-Slenderness Reinforced Concrete Walls: Design Basis and Test Results," *ACI Structural Journal*, Vol. 96, No. 4, Jul.-Aug., pp. 649-660.

Sato, S.; Ogata, Y.; Yoshizaki, S.; Kanata, K.; Yamaguchi, T.; Nakayama, T.; Inada, Y.; and Kadoriku, J., 1989, "Behavior of Shear Wall Using Various Yield Strength of Rebar, Part 1: An Experimental Study," *Proceedings*, Tenth International Conference on Structural Mechanics in Reactor Technology, H09/01, Anaheim, CA.

Soong, T. T., 2004, *Fundamentals of Probability and Statistics for Engineers*, John Wiley & Sons, Chichester, England, 391 pp.

Synge, A. J., 1980, "Ductility of Squat Shear Walls," *Report* No. 80-8, Department of Civil Engineering, University of Canterbury, Christchurch, New Zealand, 142 pp.

Wiradinata, S., 1985, "Behavior of Squat Walls Subjected to Load Reversals," MS Thesis, Department of Civil Engineering, University of Toronto, Toronto, ON, Canada, 171 pp.

Xie, L., and Xiao, Y., 2000, "Study on Retrofit of Existing Squat Concrete Shear Walls," *Report* No. USC-SERP 2000-5, Department of Civil Engineering, University of Southern California, Los Angeles, CA, 111 pp.